早稲田大学審査学位論文
博士（スポーツ科学）

The Beneficial Effects of Mechanical Stress on Disuse-Induced Skeletal Muscle Atrophy and Inflammation

不動による骨格筋の萎縮・炎症に対するメカニカルストレスの改善効果

２０１９年１月

早稲田大学大学院　スポーツ科学研究科
斎藤　久美子
SAITOU, Kumiko

研究指導教員：　鈴木　克彦　教授

CONTENTS

Chapter 1

Background

Chapter 1. Background

1.1 Mechanisms of disuse muscle atrophy

Introduction of disuse atrophy

Disuse-induced skeletal muscle atrophy occurs due to chronic periods of inactivity such as prolonged trauma, bed rest and microgravity environments [1-3]. Symptoms of skeletal muscle atrophy is mainly characterized by loss of muscle volume or mass, decreased myofiber cross-sectional area (CSA) and muscle weakness. Ogawa et al. examined myofiber CSA in quadriceps femoris muscle from healthy volunteers after 20 days of bed rest [1]. During bed rest, myofiber CSA decreased significantly by 3.7%. Haus et al. reported that simulated microgravity, utilizing either unilateral lower limb suspension, caused marked the decreases in quadriceps femoris muscle volume (35 days of unilateral lower limb suspension: −9% and 90 days of bed rest: −18%) and triceps surae muscle volume (35 days of unilateral lower limb suspension: −11% and 90 days of bed rest: −29%) [2]. Likewise, LeBlanc et al. demonstrated that significant and evident changes in muscle volume occurred in astronauts as a result of spaceflight (8 days of weightlessness): the triceps surae (-6.3%), anterior calf (-3.9%), hamstrings (-8.3%), quadriceps (-6.0%) and intrinsic back (-10.3%) muscles [3].

On the other hand, several studies have been made on disuse muscle atrophy using the rodent models [4,5]. The extent of disuse muscle atrophy shown by the decreases in gastrocnemius muscle mass amounted 15% or 25% after 7 days of hindlimb suspension or denervation, respectively [6].

Both the decrease in protein synthesis and the increase in protein degradation have been shown to contribute to muscle atrophy induced by disuse, and current works have validated elements of both protein synthetic and proteolytic processes underlying muscle atrophy. Protein turnover is varied based on changes in the modes

of muscle movement. The increase and decrease in physical activity stimulate muscle fibers to adapt, altering fiber size and protein expression. The output of these adaptive responses reflects the net balance between synthesis and degradation of proteins. Atrophy is induced when protein degradation exceeds synthesis. Therefore, we focused on muscle protein loss related to intracellular signaling during muscle atrophy.

Several proteolytic systems responsible for muscle wasting involve the ubiquitin–proteasome system, the lysosomal system and the Calpain system [7]. In disuse atrophy, the ubiquitin-proteasome system constitutes a primary signaling pathway of these metabolism, providing a mechanism for the selective breakdown of targeted proteins [8].

Overview of the ubiquitin-proteasome system

The ubiquitin-proteasome system is one of the major pathways for selective protein degradation in mammalian cells and is considered to dissolve a large amount of intracellular proteins during muscle remodeling, and to induce intracellular signaling pathways and physiological protein turnover. The system recognizes damaged and/or misfolded proteins and labels these targeted proteins by putting the polypeptide ubiquitin. Ubiquitin-tagged proteins are consequently recognized and dissolved by 26S-proteasome, a multicatalytic enzyme complex [9]. In brief, degradation of a protein by the ubiquitin system composes of two distinct and successive steps: conjugation of several ubiquitin molecules to the targeted protein and breakdown of the tagged protein by the 26S-proteasome [10].

Conjugation of ubiquitin to the targets proceeds via a three-step mechanism. Initially, ubiquitin is activated in its C-terminal Gly by the ubiquitin-activating enzyme, E1. Only one E1 protein has been discovered, an abundant 110-kDa protein

necessary for survival. Next, one of several E2 enzymes (ubiquitin-carrier proteins or ubiquitin-conjugating enzymes) interacts with one of ubiquitin ligases (E3s) to attach activated ubiquitins to the targets via a peptide bond. Dozens of E2 proteins have been discovered, indicating manifold roles of each E2 in targeting specific types of protein substrates. Finally, the targeted protein is catabolized by the 26S-proteasome complex. The 26S-proteasome breaks the substrate in small peptides (3-5 amino acid resides) via an ATP-dependent process.

The ubiquitin-proteasome system in disuse muscles

During physical activity, skeletal muscles are exposed to mechanical stress. The changes of mechanical stress yielded by muscle disuse can stimulate the ubiquitin-proteasome system activity, altering activity-related signals.

Recent studies demonstrate that the ubiquitin-regulated signals are sensitive to muscle use [11]. The same is true of conditions of decreased muscle movements that include denervation [12-14], immobilization [15] and gravitational unloading [16,8]. For example, two E3 proteins, atrogin/MAFbx and MuRF1, were elevated in the state of physical inactivity, including hindlimb immobilization, gravitational unloading and muscle denervation [12], and muscle contraction performed immediately after immobilization instigated a decline in MAFbx and MuRF1 [15]. Response of the system to changes in muscle movements appears to alter according to duration and intensity of the intervention [17-19]. The changes in system activity are anticipated to stimulate both pathway events and general proteolysis by degradation of targeted proteins [11].

The myogenic transcription factor MyoD is one of such regulations in muscles. The ubiquitin-proteasome system selectively degrades the MyoD protein, preventing

MyoD signaling [20]. Another is regulation of NF-κB signaling by the ubiquitin-proteasome system. NF-κB signaling has been appreciated as a main pro-inflammatory signaling pathway, regulating the expression of other pro-inflammatory products like cytokines and chemokines. NF-κB is up-regulated during tissue inflammation and acts also in response with other cytokines. Ubiquitin conjugation targets NF-κB inhibitor proteins, I-κB [21]. Thereby, I-κB degradation by this system causes NF-κB activation, inducing muscle wasting [4].

Collectively, the ubiquitin-proteasome system appears to relate both muscle adaptation and atrophy, mediating muscle remodeling. However, little is known how the signals were regulated during muscle use or inactivity.

1.2 Inflammation

Acute inflammation and chronic inflammation

Inflammation is the physiological response through which the body restores tissue injury and defends itself against stimuli including pathogens and noxious agents. Symptoms of inflammation are redness, swelling, heat and pain.

After the initial stimulus, abundant pro-inflammatory cells flow into the site of inflammation. The event begins with secretion of chemokines and cytokines from local cells, including neutrophils, macrophages, dendritic cells, vascular endothelial cells, and interstitial fibroblasts. Neutrophils are the first pro-inflammatory cells to arrive at the site. Neutrophils are included in restoration by causing secondary damage, through the release of reactive oxygen species (ROS) and proteases, as well as promoting phagocytosis and recruitment of monocytes by the secretion of cytokines and chemokines [22,23]. Then, monocytes reach the extravascular tissue, where they transform into macrophages. Activated macrophages (also called M1, below-

mentioned) accelerate the mobilization and the activation of pro-inflammatory effector cells, leading to the activation of NF-κB in association with a series of pro-inflammatory cytokines, such as IL-1β and TNF-α. As activated macrophages are the main producers of such pro-inflammatory cytokines, the cells play a pivotal role in onset and progression of inflammation. Activated macrophages have an enhanced capacity to phagocytose microbes, pathogens, damaged tissues and apoptotic cells, and produce also a series of biologically active molecules that facilitate myoblast proliferation, such as satellite cell. Activated satellite cells begin to proliferate, thereby providing a supply of myonuclei for the formation of new myofibers.

Subsequently, anti-inflammatory macrophages (also called M2, below-mentioned) contribute to tissue restoration, during which macrophages secrete IL-10 and transforming growth factor-ß (TGF-ß) that dampen the initial cytokine production. These cytokines also support myogenesis, promoting adequate wound healing [24]. Such a phenotype shift from pro-inflammatory to anti-inflammatory macrophages is likely induced by phagocytosis of debris [25]. Prohibition of inflammation by removal of mediators and pro-inflammatory effector cells allows the host to restore tissue damage. The usual outcome of the acute inflammatory pathway is successful resolution and repair of tissue damage, without persistence of the inflammatory conditions, which can lead to scarring and chronic loss of organ function. Acute inflammation is typically self-limiting, and the tissue is restored to the homeostatic state. Although the precise mechanisms regulating the switch from pro-inflammatory to anti-inflammatory signaling are not fully clarified, components of resolution include an apoptosis, anti-inflammatory cytokines, anti-oxidants and protease inhibitors. Notably, macrophages also play a pivotal role in this process. In acute

inflammation, if the effectors are eliminated, macrophages eventually return to steady state.

Because the resolution process involves dynamic reactions, this process may prolong and perpetuate inflammation. Disruption of mechanisms can cause incomplete recovery and sustained inflammatory conditions. The disruption was brought about by failure to eliminate the offending agents, for instance. Insufficient clearance of pro-inflammatory cells may alter functions of immune cells, affecting resolution-related signaling, and causing chronic inflammation.

Chronic inflammation is an extended inflammation, in which tissue damage and recovery coexist, leading to abnormal tissue remodeling and functional disorder. Chronic inflammation begins as a low-grade, smoldering response with no manifestation of the signs of inflammation (redness, swelling, heat and pain). However, even low-grade inflammation may damage tissue function. Moreover, the continuous progression of tissue damage and recovery promotes abnormal tissue remodeling (e.g. extensive fibrosis) that may ultimately cause irreversible tissue dysfunction [26].

A complex interplay between parenchymal cells within a tissue and the various cells in the interstitium, including immune cells, vascular cells and fibroblasts, leads the process of chronic inflammation under the influence of inputs from both the local microenvironment and the whole body. In particular, the attention is paid to monocyte/macrophage lineage cells, which act as major effector cells in chronic inflammatory pathways during the pathological development [26].

A primary function of macrophages for recovery from inflammation is the clearance of effector cells (especially apoptotic granulocytes [27]) and pathogens). Insufficient clearance of pro-inflammatory molecules by macrophages may also block

resolution, affecting resolution-related signaling and processes. In summary, the diminished macrophage phagocytic activity results in accumulation of damage-associated molecular patterns (DAMPs), eventually resulting in chronic inflammation. More researches are needed to determine how inflammation causes loss of phagocytic functionality of macrophages in future studies.

1.3 Atrophy and inflammation

The association between disuse muscle atrophy and inflammation remains controversial. Some studies reported that pro-inflammatory cytokine, TNF-α [28-31], interferon (IFN)-γ and IL-1 [31] increase ubiquitin-conjugating activity in skeletal muscle. In contrast, some studies proposed that ubiquitin-proteasome system facilitates to activation and translocation of NF-κB, as well as a feed-forward signal that promotes expression of genes for ubiquitin, E2/E3 proteins and proteasome subunits [32-36].

It also has been reported that physical activity can lead to mitigation of systemic inflammation due to a decrease in pro-inflammatory mediator [37,38], and that exercise suppresses infiltration of pro-inflammatory macrophages and CD8 T cell [39], suggesting that disuse muscle atrophy and inflammation may interact each other. One thing for sure, that is, disuse muscle atrophy and inflammation exist and link together in muscle tissues. Additional work is needed to confirm the association between atrophy and inflammation.

1.4 The role of macrophages in inflammation

Origin of macrophages

Macrophages derive from three sources. The first is the yolk sac in the embryo, where F4/80^{high} macrophage progenitors are yielded. Later during fetal development, the production of hematopoietic stem cells shifts to the second source, fetal liver. The third source is the bone marrow, which gives rise to monocytes. When incompletely differentiated monocytes reach the extravascular tissue, they transform into monocyte-derived macrophages.

Macrophages exist in all organs and connective tissues and are named as suitable for their location, such as microglial cells, osteoclasts, alveolar macrophages and Kupffer cells. In addition to macrophage heterogeneity in different organs and tissues, macrophage can exhibit heterogeneity within a single organ or tissue. Moreover, in the case of inflammation-related macrophages, after cells have differentiated in a microenvironment, whether they are then terminally differentiated, or whether they are functionally flexible and able to adapt their phenotype in response to changes in their location, have not been brought out yet. According to a previous report, most macrophages in the adult tissues have been considered to be derived from blood monocytes, which homeostatically replenish tissue-resident macrophage populations [40]. However, studies about the origins of many tissue-resident macrophages have proposed that local proliferation has a conceivable way in the renewal and maintenance of tissue-resident macrophages [41,42].

Macrophages were found to invade atrophied myofibers in unloaded soleus muscle [43]. Because macrophages produce multiple biological molecules involved in both pro-inflammation and anti-inflammation, medical interventions targeting macrophages and their products may open new gateways for regulating skeletal muscle atrophy and inflammatory diseases.

Chemokine family

For monocytes/macrophages recruitment, the release of monocyte chemoattractant protein-1 (MCP-1), a member of chemokine family, is enhanced in damaged skeletal muscle. Chemokines are typically released by pro-inflammatory cells, and are thought to provide the directional cues for the movement of monocytes/macrophages in inflammation [44], which influences the activation state of immune cells. These signaling molecules are classified according to the number and distribution of cysteine residues near their amino terminus, being named as C, CC, CXC or CX_3C chemokines. They show variable specificity and reflect some overlap of functions. Following muscle injury and disease, chemokines and their receptors are expressed in a mass, suggesting that they may be essential in muscle regeneration [45,46].

M. Brigitte et al. have shown that large amounts of monocytes/macrophages that are recruited into muscle at the time of trauma from a muscle tissue compartment, the epimysium/perimysium. This study has shown that the resident macrophages of skeletal muscle exist in epimysium/perimysium and that they release MCP-1 on muscle injury. Resident macrophages play a key role in the subsequent recruitment of circulating monocytes to the damage cite [47].

Functions of macrophages

Macrophages are a major cell of the mononuclear phagocyte system that consists of related cells of bone marrow origin, including circulating monocytes. During inflammation, macrophages have three major function; (1) antigen presentation, (2) phagocytosis and (3) immunomodulation, through production of various cytokines and transforming growth factors [48]. Macrophages are crucial for the initiation, persistence and resolution of inflammation due to being activated and deactivated in

the inflammatory pathway. Activated macrophages are deactivated by anti-inflammatory cytokines (e.g. IL-4, IL-10, IL-13 and TGF-β) and cytokine antagonists that are produced by macrophages. Macrophages engage in the autoregulatory loop in the inflammatory pathway.

(1) Antigen Presentation

Macrophages act to display antigens for recognition by T lymphocytes and to stimulate the activation of T lymphocytes as antigen-presenting cells. Antigen-presenting cells include dendritic cells and monocytes/macrophages. The macrophage-cytokine-T lymphocyte axis plays a pivotal role in development of adaptive immunity against intracellular pathogens.

(2) Phagocytosis

Macrophages intake materials to eliminate waste and debris and to kill invading pathogens. Macrophages express receptors, such as scavenger receptors, mannose receptors, Toll-like receptors (TLRs), seven α-helical transmembrane/G protein-coupled receptors and receptors for opsonin. Those receptors exhibit functions by recognizing and binding pathogens, and macrophages can intake them [49].

(3) Immunomodulation

Activated macrophages secrete cytokines, such as TNF-α, IL-1, IL-6, IFN-α/ß, IL-10, IL-12, IL-18, MCP-1, CX3CL1, urokinase and vascular endothelial growth factor. These molecules include in the regulation of immune/inflammatory responses. For example, IL-12 is a heterodimeric cytokine released primarily by antigen-presenting cells that have important influences in the regulation of the inflammatory pathway. IL-12 promotes proliferation of activated T lymphocytes and natural killer (NK) cells, stimulates lytic activity of cytotoxic T lymphocytes, and induces IFN-γ production by T lymphocytes and NK cells. IL-12 plays a main role in accelerating type 1 helper T

lymphocyte (Th1) immune responses and adaptive immunity [50]. That is, IL-12 acts a functional bridge between the early nonspecific innate immunity and the following antigen-specific adaptive immunity [51]. In addition, one of chemokines, MCP-1, stimulates migration of immune cells from the blood to tissues [52].

Classification of macrophage populations: macrophage polarization in tissue repair

Macrophages are present as functionally different populations at different times during acute inflammation. In general, these populations are assumed to exhibit conflicting functions, being either polarized towards pro-inflammatory or anti-inflammatory activity [53]. Polarized macrophages are currently categorized as either M1 or M2, referring to either classical or alternative activation [54,55]. Despite this dichotomy being, it is important that the M1/M2 dichotomy is not sufficiently established, and that the categorization of macrophages into these two groups is often ambiguous. Pro-inflammatory M1 macrophages emerge from exposure to cytokines, IFN-γ and TNF-α, in addition to bacterial lipopolysaccharide (LPS) or endotoxin [55,56]. On the other hand, polarization of M2 macrophages is complex, including three possible subtypes. However, those exact properties are not elucidated. Alternative M2a macrophages are commonly involved in advanced stages of tissue restoration and wound healing, and arise from exposure to cytokines, such as IL-4 and IL-13. M2b macrophages also have an anti-inflammatory function and can secrete large amounts of IL-10. IL-10 is known to give rise to M2c macrophages which have an anti-inflammatory function. Therefore, M2b also share many functions with tumor associated macrophages [57].

Pro-inflammatory M1 macrophages are found in the context of muscle repair at early stages after muscle damage, followed by macrophages having characters with the anti-inflammatory M2 phenotype [53]. In an early stage, M1 macrophages phagocytose necrotic cell debris and accomplish the processing and presentation of antigens. In addition to releasing large amounts of pro-inflammatory cytokines, M1 macrophages also secrete inducible nitric oxide synthase (iNOS), which is required for killing intracellular pathogens. Alternative activated M2 macrophages exist in large quantity during the final phase of tissue repair [58], suggesting that a wide range of M2 macrophage subtypes might act during the muscle repair process.

Despite the emergence of convincing evidence for the presence of different macrophage populations and subtypes in muscle repair, a clear comprehension of their specific functions is still lacking. Furthermore, the mechanisms in regulating cytokine gene silencing and macrophage deactivation have not been completely explained yet.

1.5 Massage therapy

Massage as an alternative medicine

Massage therapy is one of the most widely accepted alternative intervention. Recently, there has been an expansion in the usage of alternative medicine, and massage is appreciated by a large number of people [59]. Massage may be a safe and beneficial interventions devoid of any major risks or side effects if rendered by trained professionals [60]. Massage can produce mechanical stress, which is expected to increase muscle extensibility. However, despite its increasing popularity, there remains controversial in the effectiveness of massage as a complementary medicine.

Types of massage

Massage has been defined as “a mechanical manipulation of body tissues with rhythmical pressure and stroking for the purpose of promoting health and well-being” [61]. There are several techniques in existence, and their use depends on the experience of the professional and the intended advantage [62-65]. Massage has long been considered to relate to physiological, biomechanical, neurological and psychological mechanisms [66,67]. So far, majority of these mechanisms are speculated that the possible increase in muscle blood flow, as well as the possible decrease in neuromuscular excitability, which are occurred from mechanical stress, may be factors in any benefits of massage on muscle adaptation. Meanwhile, it has been reported that massage does not alter blood flow for brachial and femoral arteries [68,69], and femoral vein [69]. Inferences on the possible factors are needed for further research to develop the true mechanisms and benefits of massage.

Mechanisms of massage

Various physiological factors are affected through massage. It is obvious that it begins from the mechanical stress occurred from various therapy techniques. When certain kind of mechanical stress is applied to living cells, a complex array of sensors on the surface of the cells are capable to sense and adapt to the stress. Mechanical stress applied to those sensors activates several kinases such as focal adhesion kinase (FAK) and the mitogen-activated protein kinase (MAPK) family of proteins. These sets of kinases play further role in eliciting expression of regulatory factors that modulate protein synthesis, glucose uptake and immune cell recruitment [70-72]. Thus, massage applied to body with a systematic mechanical stress varies degree of signaling cascade, introducing a positive effect. However, it is unclear what cells are sensitive to mechanical stress evoked by massage.

1.6 The relationship between massage and immune system

Intensive exercise is responsible for producing small tears in muscle fibers, thereby, leading inflammation and soreness [73,74]. Crane et al. found that massage down-regulated the production of NF-κB and pro-inflammatory cytokines TNF-α, thereby, mitigating the cellular stress arising from exercise-induced muscle damage [75]. However, little attention has been given to the effects of massage on disuse-induced inflammation.

Besides, massage also has influence on lymph dynamics. Proper lymph dynamics are important for effective immune system. Lymphatic system plays a crucial role in fighting infection and in drainage of lactic acid, cell debris, excess interstitial fluid and intestinal toxins from tissues, and the same is said to be positively influenced by massage therapy [76-78]. It was reported that combination of manual lymphatic drainage and the therapeutic ultrasound evidently modulated the swelling and tissue fibrosis [79].

Massage may have a connection with immune system. Consequently, although the connection between massage and ubiquitin-proteasome system for promoting disuse muscle atrophy is not still clarified, it is quite likely that abrogation of tissue inflammation due to massage allows inhibition of disuse muscle atrophy.

1.7 Research objective

Physical inactivity, the 4th leading risk factor for death worldwide, kills more than 5 million people every year [80]. It arises from a variety of health problems including ageing, injury and neuromuscular diseases, and can lead to numerous organismal disorders such as muscle atrophy [81]. Inflammation, which involves enhanced

expression or production of pro-inflammatory cytokines and chemokines, has been implicated in the pathology of disuse muscle atrophy [82, 83]. In addition to the chronic nature of inactivity-related inflammation [84], a vicious circle formed by physical inactivity and muscle weakness exacerbates loss of muscle mass, resulting in irreversible deterioration of general bodily functions.

Physical exercise has anti-inflammatory effects [37, 85]. However, the molecular mechanisms underlying the benefits of exercise to organismal homeostasis are poorly understood, especially in respect to its suppression of local inflammation. This problem may partially account for the small population partaking in habitual exercise [86, 87] and the lack of guidelines for physical exercise as a therapeutic/preventative intervention in lifestyle-related diseases and disorders including muscle atrophy.

Massage is generally appreciated as a pain- or inflammation-relieving procedure, being recognized to be beneficial for pain relief and improvement of physical performance for both competitive athletes and non-athletes alike [88, 89]. In fact, massage reportedly suppresses local inflammation [90] and prompts recovery from exercise-induced muscle damage [75, 91]. Although little is known about the biochemical mechanisms behind the benefits of massage, there is a common feature between physical exercise and massage. They both generate local mechanical stress on organs, tissues and cells. Taken together with the anti-inflammatory effects of both exercise and massage [75, 92, 93], we hypothesized that mechanical stress generated by massage or massage-like interventions might modulate local inflammatory processes underlying disuse muscle atrophy.

Macrophages play important roles in the regulation of various immune responses and inflammatory processes [94, 95]. In the context of organismal homeostasis, macrophages are critically involved in many age-related disorders including diabetes

mellitus [96], atherosclerosis [97], Alzheimer's disease [98] and cancer [99]. The research objective of this thesis is to elucidate our hypothesis, whether mechanical stress generated by massage or massage-like interventions might modulate local inflammatory processes underlying disuse muscle atrophy. In the case that this hypothesis is revealed, the mechanisms coexisted among physical activity and massage may be identified, and a cue to develop massage as an alternative intervention to exercise may be provided.

Chapter 2

The modulation of macrophage functions *in situ* and the alleviation of immobilization-induced muscle atrophy and inflammation by local cyclical compression (LCC)

2.1 Objective

To test whether massage-like mechanical interventions could modulate disuse muscle atrophy and inflammation of immobilized skeletal muscles, we conducted the LCC-applied experiments.

For promoting disuse muscle atrophy *in vivo*, various models have been used, however they are also suffered from invasive surgical and special devices for immobilization. Here, we adopted an animal model of disuse muscle atrophy that we previously developed [100]. At first, we examined whether mouse hindlimb immobilization by spiral wiring induced local inflammatory responses and muscle atrophy. Next, we applied LCC, mimicking massage, on unilateral calf muscles of mice with coiled bilateral hindlimbs and analyzed right-left differences in efficiency of LCC.

2.2 Materials and methods

Animals

All animal experiments were approved by the Institutional Animal Care and Use Committee of National Rehabilitation Center for Persons with Disabilities. C57BL/6J mice purchased from Charles River Laboratories (Yokohama, Japan) were housed with free access to water and standard rodent chow under a 12-h light/dark cycle at 22 ±2℃ and constant humidity (55±10%). Male mice were subjected to experiments at the age of 11-12 weeks after an acclimation for at least 7 days.

Antibodies and chemicals

Rat monoclonal anti-laminin-2 antibody (Cat# L0663) was purchased from Sigma-Aldrich (St. Louis, MO). Rat monoclonal anti-F4/80 antibody (Cat# ab6640), rabbit

polyclonal anti-MCP-1 antibody (Cat# ab25124) and rabbit polyclonal anti-TNF-α antibody (Cat# ab66579) were purchased from Abcam (Cambridge, UK). Goat anti-rabbit Alexa Fluor 488 (Cat# A11034) and goat anti-rat Alexa Fluor 568 (Cat# A11077) were purchased from Invitrogen (Carlsbad, CA). Clodronate liposome (Clophosome-A) and its control liposome were purchased from FormuMax Scientific (Sunnyvale, CA). Sodium pentobarbital was purchased from Kyoritu Seiyaku (Tokyo, Japan). The other chemicals were purchased from Sigma-Aldrich unless noted otherwise.

Immobilization of mouse bilateral hindlimbs

Bilateral hindlimbs of mice were immobilized as described previously [100]. Surgical tape (3M Japan, Tokyo, Japan) and aluminum wire (Eko Metal, Niigata, Japan) were applied to mice under hypnosis with sodium pentobarbital (50 mg/kg i.p.) so that the motions of their bilateral hindlimbs were restricted with their hip joints abducted, knee joints extended and ankle joints plantar-flexed for defined periods (Figure 1A).

LCC on mouse calves

Hindlimb-immobilized mice were hypnotized with sodium pentobarbital, temporarily disengaged from wiring, and laid at a prone position with their knee joints extended and ankle joints plantar-flexed so that their calves faced upward. LCC was applied by vertically moving a cylindrical weight unit covered with a cushion pad (Figure 1B). After LCC application for 30 min, mouse hindlimbs were re-coiled to continue immobilization (Figure 1C). Among the several different LCC magnitudes we tested by changing the weight of the cylindrical unit (Figure 2A), the one that produced 50 mmHg intramuscular (gastrocnemius) pressure waves (Figure 2B) appeared to be

optimal in terms of alleviation of immobilization-induced muscle atrophy and local macrophage accumulation. We also confirmed that LCC of this mode/magnitude did not generate apparent muscle damage at a microscopic level (Figure 2C). We therefore employed this LCC set-up for further studies. LCC side (right or left) was chosen randomly.

Selective depletion of monocytes/macrophages recruited from circulating blood

To deplete phagocytic cells recruited from circulating blood, mice were administered with clodronate liposome according to the manufacturer's instructions, i.e. 200 µl i.p. for single administration [101], and the first 150 µl i.p. followed by 100 µl i.p. every 3 days for repeated administration [102]. Clodronate liposome (or control liposome) injection during the period of hindlimb immobilization was carried out just before re-wiring mouse hindlimbs, which had been temporarily disengaged from immobilization for the purpose of daily LCC application (Figure 3A).

Morphological analysis of blood cells

Circulating blood was collected in a tripotassium EDTA-containing tube (Terumo, Tokyo, Japan) from the inferior vena cava of mice anesthetized with intraperitoneal injection of a mixture of three anesthetic agents (medetomidine 0.75 mg/kg, midazolam 4.0 mg/kg, butorphanol 5.0 mg/kg). A thin smear of blood on a slide was dried, fixed in methanol and subjected to Wright-Giemsa staining [103] using Wright's (Muto Pure Chemicals, Tokyo, Japan) and Giemsa's (Nacalai Tesque, Kyoto, Japan) solutions diluted with pH6.4 phosphate buffer (LSI Medience, Tokyo, Japan). Differential counting was conducted for 100 white blood cells in each sample.

Immunohistochemical analysis of calf muscle tissues

Immediately after euthanizing mice by cervical dislocation, triceps surae muscles were dissected, quickly frozen in an optimal cutting temperature compound solution (Sakura Finetek, Torrance, CA), and subjected to cryostat (CM3050 S, Leica Biosystems, Eisfeld, Germany) sectioning with 20 μm thickness. Specimens mounted on glass slides were incubated in blocking buffer (Protein Block Serum-Free, Dako, Carpinteria, CA) for 30 min at room temperature, and then with primary antibodies overnight at room temperature followed by Alexa Fluor 488- or 568-conjugated secondary antibodies for 1 h at room temperature. Both primary and secondary antibodies were diluted in a Tris-HCl buffer (REALTM Antibody Diluent, Dako, Carpinteria, CA). Nuclei were counterstained with DAPI (Thermo Fisher Scientific, Waltham, MA). After mounting with an antifade reagent (Prolong Gold, Thermo Fisher Scientific), specimens were viewed using a fluorescence microscope (BZ-9000, Keyence, Osaka, Japan).

Histomorphometrical analysis of muscle tissues

Mouse calf muscles were histomorphometrically analyzed at their 1/3 proximal levels, where their bellies appeared thickest. The CSA of each myofiber was determined by tracing the ‘internal’ margin of the basement membrane visualized with anti-laminin-2 immunostaining (cyan dot line in Figure 3B). Interstitial space surrounding individual myofiber was defined by tracing the ‘external’ margin of the basement membrane (yellow dot line in Figure 3B). Microscopic images were analyzed using ImageJ software (NIH, Bethesda, MD). Cells positively stained with F4/80, a marker for macrophage [104], were defined as macrophages.

Measurement of intramuscular pressure of mouse gastrocnemius muscles

Under anesthesia with intraperitoneal injection of a mixture of three anesthetic agents, 11-12-week old male mice were subjected to intramuscular pressure measurement. Through a posterior skin incision on the calf, a 20-gauge indwelling needle was inserted to the gastrocnemius muscle at an obtuse angle. Using its plastic sheath as a guide, a sensor of blood pressure telemeter (Millar, Houston, TX) was placed in the mid-belly of the muscle. After suturing the skin, intramuscular pressure was monitored using LabChart8 (ADInstruments Japan, Nagoya, Japan).

Measurement of contracting forces of mouse triceps surae muscles

Triceps surae muscle contracting forces were measured by the electrical stimulation method that we reported previously [105]. Under anesthesia with a mixture of three anesthetic agents (i.p.), 11-12-week old male mice were placed in a prone position with their unilateral feet on a footplate fixed on a rotatory disc (knee joint extended and ankle joint at 90 degrees) to quantify the torques. A surface electrode connected to an electric stimulator and an isolator (SS-104J; Nihon Kohden, Tokyo, Japan) was attached on their pelage-cleared calves to induce their triceps surae muscles to contract isometrically. We defined the muscle contracting forces as the torques generated at the maximal tetanic contractions (peak tetanic torques) elicited by the electrical stimulation with rectangular pulses (duration; 4 msec, frequency; 100 Hz). The stimulation intensity for the maximal contraction, which was determined by varying single stimuli in each sample, ranged from 15 to 20 V.

Statistical analysis

Data are presented as means ± S.D. Multiple group comparison was performed by ANOVA with post hoc Bonferroni procedure unless noted otherwise. $P < 0.05$ was considered statistically significant.

Abbreviations

CSA, cross sectional area; CDN, clodronate; LCC, local cyclical compression; MCP-1, monocyte chemoattractant protein-1; TNF-α, tumor necrosis factor-α.

2.3 Results

Mouse hindlimb immobilization by spiral wiring induces atrophy and inflammatory responses of calf muscles

We first examined whether mouse hindlimb immobilization by spiral wiring, an animal model of disuse muscle atrophy that we previously developed [100], induced local inflammatory responses. Consistent with our previous observations, both the muscle mass of triceps surae and the cross-sectional area (CSA) of gastrocnemius myofibers were significantly decreased by hindlimb immobilization (Figures 4A-4C). Given no apparent damage or injury observed in muscle tissues of immobilized hindlimbs (Figure 2C), these results indicate that calf muscles were atrophied by immobilization. Immunofluorescence staining revealed that cells expressing MCP-1 and TNF-α, both of which play key roles in regulating inflammatory processes [44, 106], and cells positively stained with F4/80, a marker for macrophages, significantly increased in gastrocnemius muscle tissues of immobilized hindlimbs (MCP-1; Figures 5A, 5D and 5F, TNF-α; Figures 5B, 5E and 5G, F4/80; Figures 5A-5C, 5F and 5G).

LCC attenuates immobilization-induced muscle atrophy with a modulation of inflammatory responses

We next examined whether massage-like mechanical interventions could modulate the pro-inflammatory effect of hindlimb immobilization on calf muscles. When we applied LCC (1 Hz, 30 min/day, Figure 1C) on mouse calves during the period of hindlimb immobilization, the CSA of gastrocnemius myofibers became significantly larger as compared to that in their contralateral control hindlimbs left unexposed to LCC (Figures 6A and 6B). Furthermore, LCC partially tempered the immobilization-induced decrease in contracting forces of triceps surae muscles (Figure 6D). In contrast, the muscle mass of triceps surae was not significantly different between immobilized hindlimbs with and without LCC application (Figure 6C). Because we observed a decrease of the interstitial space in LCC-applied gastrocnemius (Figures 7A and 7B), we speculate that LCC tempered immobilization-induced edematous reactions of muscle tissues [107]. This in turn may have obscured the positive effects of LCC on muscle mass measured as a total wet tissue weight. In addition, LCC decreased the numbers of F4/80-positive, TNF-α-positive, and F4/80- MCP-1- or TNF-α- double positive cells in gastrocnemius muscle tissues of immobilized hindlimbs (F4/80; Figures 8A-8C, 8F and 8G, MCP-1; Figures 8A, 8D and 8F, TNF-α; Figures 8B, 8E and 8G).

Depletion of macrophage recruited from circulating blood eliminates immobilization-induced muscle atrophy and inflammatory responses

The expression of MCP-1, which plays a crucial role in recruiting monocytes/macrophages from circulating blood [44], significantly increased prior to the decrease in both muscle mass and myofiber CSA upon immobilization (Figures

4B, 4C and 5D). Furthermore, MCP-1 expression increased more rapidly than that of TNF-α during the period of hindlimb immobilization (compare Figures 5D and 5E). Taken together, these results suggest that macrophage accumulation precedes muscle atrophy upon immobilization. We then asked whether this macrophage accumulation was due to the recruitment from circulating blood or proliferation/differentiation of local macrophages and their precursors, or both. To test this, we conducted hindlimb immobilization experiments using mice administered with clodronate liposomes (Figure 3A). Clodronate liposomes induce apoptosis of phagocytic cells but cannot cross the capillary wall, thereby depleting circulating monocytes and newly-recruited macrophages (Figure 9A) but not muscle-resident macrophages or their precursors [108]. In clodronate liposome-administered mice, we did not observe significant decrease in the muscle mass of triceps surae and the CSA of gastrocnemius myofibers after hindlimb immobilization (Figures 9B-9D, compare columns 2 and 5 in Figures 9C and 9D). Furthermore, hindlimb immobilization did not significantly increase the interstitial space in gastrocnemius muscles of those mice (compare columns 2 and 5 in Figure 9E). Notably, the effects of daily LCC on the CSA of gastrocnemius myofibers (Figure 9D), the numbers of F4/80-, MCP-1-, and TNF-α-positive cells *in situ* (F4/80; Figures 10A, 10B, 10D, 11A and 11C, MCP-1; Figures 10A, 10C and 10D, TNF-α; Figures 11A-11C), and the gastrocnemius interstitial space (Figure 9E) in immobilized hindlimbs were eliminated by clodronate liposome administration (compare columns 5 and 6 in each graph).

The number of F4/80-positive cells did not decrease in gastrocnemius muscles of mice injected with clodronate liposomes three times over 8 days (compare columns 1 and 2 in Figure 10B). This might be due to proliferation of macrophages derived from local precursors during prolonged clodronate liposome treatment [109]. In line with

this, the number of F4/80-positive cells in gastrocnemius muscles was moderately increased by hindlimb immobilization even in clodronate liposome-administered mice (Figures 10A and 11A, compare columns 2 and 5 in Figure 10B).

2.4 Discussion

Together with the decreases in both the muscle mass of triceps surae and the CSA of gastrocnemius myofibers (Figures 4A-4C) and the increase in cells positively stained with MCP-1, TNF-α and F4/80 (MCP-1; Figures 5A, 5D and 5F, TNF-α; Figures 5B, 5E and 5G, F4/80; Figures 5A-5C, 5F and 5G), hindlimb immobilization appeared to instigate calf muscle atrophy involving local inflammatory responses including macrophage accumulation.

When we applied LCC on mouse calves during the period of hindlimb immobilization, the decreases in the CSA and contracting forces of triceps surae muscles were alleviated (Figure 6A, 6B and 6D). In addition, LCC decreased the numbers of F4/80-positive, TNF-α-positive, and F4/80- MCP-1- or TNF-α- double positive cells in gastrocnemius muscle tissues of immobilized hindlimbs (F4/80; Figures 8A-8C, 8F and 8G, MCP-1; Figures 8A, 8D and 8F, TNF-α; Figures 8B, 8E and 8G). Collectively, LCC alleviated local inflammatory responses including macrophage accumulation, and immobilization-induced muscle atrophy. Notably, MCP-1 expression in intramuscular macrophages appeared to be enhanced by immobilization whereas this effect was tempered by LCC (Figure 8A and 8F). In contrast, TNF-α expression in macrophages was not significantly altered by immobilization or LCC (Figure 8B and 8G).

Next, to test whether macrophage accumulation caused disuse muscle atrophy and inflammation, we conducted hindlimb immobilization experiments using mice

administered with clodronate liposomes (Figure 3A). In clodronate liposome-administered mice, the macrophage infiltration was not promoted, and disuse muscle atrophy and inflammation in immobilized gastrocnemius muscles were not occurred. Accordingly, the preventive effects of LCC towards disuse muscle atrophy and inflammation was eliminated. These results suggest that macrophages recruited from circulating blood, but not those derived from local precursors, play an important role in immobilization-induced muscle atrophy and inflammation.

Chapter 3

Analysis of interstitial fluid dynamics, and simulative calculation of LCC-induced fluid shear stress on cells distributed in the interstitium of gastrocnemius muscle tissues

3.1 Objective

In muscle tissues, macrophages are distributed in their interstitial space. In addition to the intramuscular pressure waves (Figure 2A), our LCC procedure was most likely to generate interstitial fluid flow, leading to shear stress exertion on interstitial cells including macrophages. To estimate the effect of LCC on the interstitial fluid dynamics, we conducted μCT imaging using an iodine-based contrast medium (Isovist) injected to gastrocnemius muscle bellies (Figure 12).

3.2 Methods

Animals

All animal experiments were approved by the Institutional Animal Care and Use Committee of National Rehabilitation Center for Persons with Disabilities. C57BL/6J mice purchased from Charles River Laboratories (Yokohama, Japan) were housed with free access to water and standard rodent chow under a 12-h light/dark cycle at 22±2°C and constant humidity (55±10%). Male mice were subjected to experiments at the age of 11-12 weeks after an acclimation for at least 7 days.

Chemicals

Isovist inj.300 was purchased from Bayer (Berlin, Germany). The other chemicals were purchased from Sigma-Aldrich unless noted otherwise.

LCC on mouse calves

Mice were hypnotized and were laid at a prone position with their knee joints extended and ankle joints plantar-flexed so that their calves faced upward. LCC was

applied by vertically moving a cylindrical weight unit covered with a cushion pad (Figure 1B). LCC side (right or left) was chosen randomly.

μCT imaging of the dynamics of intramuscular interstitial fluid

11-12-week old male mice anesthetized with a mixture of three anesthetic agents (i.p) were subjected to microinjection of an iodine-based contrast medium (Isovist® inj. 300), followed by μCT imaging. After exposing fascia through 2-mm posterior skin incision on the calf, a 31-gauge needle was inserted to the depth of 2 mm to locate its bevel tip in the mid-belly of gastrocnemius muscle. Using a microsyringe (Microliter Syringe, Hamilton, NV) and a stereotaxic injector (Legato130, Muromachi, Tokyo, Japan), 3 μl of contrast medium was infused with the rate fixed at 0.6 μl/min. After completing the infusion, we held the microsyringe for 5 min to avoid reflux, pulled out the needle carefully, closed the skin with a tissue adhesive (3M Vetbond, St. Paul, MN), and set the mice in a CT scanner (inspeXio SMX-100CT, Shimadzu, Kyoto, Japan). Mice were subjected to two serial hindlimb μCT scans between which LCC was either applied or left unapplied (kept sedentary) for 5 sec (Figure 12A). μCT images were obtained with following parameters; voxel size 50 μm, 60 KeV, 58 μA, field of view 25.6 mm, matrix size 512 x 512 (Figure 12B). 3D reconstructed objects were visualized and analyzed on software for 3D histomorphometry (TRI/3D-BON-FCS64, RATOC System, Tokyo, Japan). The contrast medium cluster in muscle belly was defined as voxels with ≥1.2 times signal intensity as compared to that of muscle parenchyma (Figure 13A).

Simulative calculation of the magnitude of interstitial fluid flow-derived shear stress during LCC

Based on measurements of the spreading of contrast medium, we calculated the velocity of interstitial fluid movement induced by LCC. We assumed that interstitial fluid flow in the muscle tissue follows the Henry Darcy's law, which defines the flux density of penetrating fluid per unite time. The velocity of interstitial fluid flow (u) is assumed to approach the superficial velocity (u_∞) and zero ($u = 0$) at the cell surface (*i.e.* a no-slip condition). Using these two boundary conditions together with the Brinkman equation, fluid shear stress (τ) at the cell surface can be obtained as described in Table.

Statistical analysis

Data are presented as means ± S.D. Statistical comparison between two groups was performed by Student's t test. $P < 0.05$ was considered statistically significant.

3.3 Results

The spreading of contrast medium was dominantly observed along the direction of myofibers (Figure 13A). We therefore compared the longitudinal distances of contrast medium spreading between two serial μCT images of mouse hindlimbs with and without LCC application and evaluated LCC-induced displacement of contrast medium (Figure 13B). We found that LCC prompted interstitial fluid movement with a velocity of ~50 μm/s, indicating that intramuscular macrophages were subjected to FSS derived from interstitial flow during LCC.

3.4 Discussion

Using parameters including the amplitude of intramuscular pressure waves that we applied (Figure 2A) and the interstitial fluid viscosity reported previously [110, 111],

our simulative calculation suggests that intramuscular macrophages or other interstitial cells might be exposed to FSS with an average magnitude of 0.94 – 1.18 Pa during LCC (Table).

Chapter 4

The reproduction of the LCC effect on MCP-1 expression *in vivo* due to FSS, but not hydrostatic pressure (HP), on macrophage *in vitro*

4.1 Objective

To examine whether the responses of macrophage to LCC *in vivo* were mechanically relevant, we exposed cultured macrophages to pulsatile FSS or HP. We used thioglycolate-elicited peritoneal macrophages, which are enriched with monocyte-derived cells [112], because LCC appeared to modulate the function of macrophages recruited from circulating blood (Figure 10 and 11). Considering LCC tempered the immobilization-induced increase in MCP-1 expression in macrophages *in situ* (Figure 8F), we tested the response of macrophages treated with LPS, which promotes M1 polarization with enhanced MCP-1 expression [113].

4.2 Materials and methods

Animals

All animal experiments were approved by the Institutional Animal Care and Use Committee of National Rehabilitation Center for Persons with Disabilities. C57BL/6J mice purchased from Charles River Laboratories (Yokohama, Japan) were housed with free access to water and standard rodent chow under a 12-h light/dark cycle at 22±2℃ and constant humidity (55±10%). Female mice were subjected to experiments at the age of 8-10 weeks after an acclimation for at least 7 days.

Isolation of peritoneal macrophages

Mouse peritoneal macrophages were isolated as described previously [114, 115]. Briefly, 3 days after 8-10-week-old female C57BL/6J mice were administered with 5 ml of Brewer thioglycolate medium (3% w/v in distilled water, i.p.), their peritoneal cavities were filled with cold 5 ml PBS, and then kneaded gently for 3 min. Injected PBS was collected using a 21-gauge needle, and the suspensions were centrifuged at

100 x *g* for 5 min to sediment a cell pellet. Cells were resuspended in RPMI-1640 (Thermo Fisher Scientific) containing 10% fetal bovine serum (GE Healthcare, Uppsala, Sweden) and seeded on a plastic dish. After 24 h, non-adherent cells were removed by two-times wash with PBS. Consistent with previous reports [116], we confirmed that 70-80% of remaining adherent cells were positive for F4/80.

Application of FSS or HP to cultured macrophages

Mouse peritoneal macrophages pre-treated with LPS (100 ng/ml) for 24 h were exposed to pulsatile FSS with an average magnitude of 0.5 Pa at a frequency of 0.5 Hz for 30 min using a custom-made flow system as described previously [117] with slight modifications. A flow-chamber, which was composed of a cell culture dish, a polycarbonate I/O unit, and a silicone gasket, generated a 22.5-mm-wide 35-mm-long 0.5-mm-high flow channel (Figure 14A). Macrophages were seeded at a density of 4 x 10^5 cells/8.0 cm^2. The system was adjusted to generate pressure waves with amplitude of 50 mmHg (zero to peak), and placed in a CO_2 incubator to maintain pH and temperature of culture medium.

As a control for FSS, macrophages seeded at a density of 3 x 10^5 cells/6.6 cm^2 were exposed to pulsatile HP with amplitude of 50 mmHg (zero to peak) at a frequency of 0.5 Hz for 30 min using a custom-made pressure system described previously [118] with slight modifications. The system consists of a cell culture dish, a polycarbonate pressure chamber, a silicone gasket, an O-ring, a quartz glass, two holding jigs, a thermostatic chamber, and a syringe pump (Figure 14B). The entire system was completely airtight, enabling precise and strict pressure control with the syringe pump. In both FSS and HP experiments, cell adhesion and morphology were observed using a light microscope (DM IRE2, Leica Microsystems, Wetzlar, Germany).

RNA extraction and real-time quantitative PCR

Six hours after the termination of FSS or HP application, peritoneal macrophages were subjected to total RNA extraction using guanidine thiocyanate (ISOGEN, Nippon Gene, Tokyo, Japan) followed by reverse transcription using both oligo(dT) and random hexamers as primers (PrimeScript RT Reagent Kit, Takara Bio, Shiga, Japan) to generate cDNA. We subjected cDNA to real-time quantitative PCR reactions in duplicates using a thermal cycler (ABI Prism 7500, Applied Biosystems, Foster City, CA). Data were analyzed using sequence detection system software (7500 System SDS, Applied Biosystems, Foster City, CA) and relative mRNA abundance was normalized to GAPDH. ΔΔCt method was applied for comparison of expression levels. The sequences of the primers used in study were as follows.

Gapdh; 5'-TGCACCACCAACTGCTTAGC-3' (forward) and

5'- GGATGCAGGGATGATGTTCT-3' (reverse),

Mcp-1; 5'-GCTCTCTCTTCCTCCACCAC-3' (forward) and

5'-GCTTCTTTGGGACACCTGCT-3' (reverse),

Tnf-α; 5'-CCTGTAGCCCACGTCGTAG-3' (forward) and

5'-GGGAGTAGACAAGGTACAACCC-3' (reverse),

Tgf-β1; 5'-AAGTTGGCATGGTAGCCCTT -3' (forward) and

5'-GCCCTGGATACCAACTATTGC-3' (reverse),

Cd206; 5'-TTCAGCTATTGGACGCGAGG-3' (forward) and

5'- GAATCTGACACCCAGCGGAA-3' (reverse).

Statistical analysis

Data are presented as means ± S.D. Statistical comparison between two groups was performed by Student's t test. $P < 0.05$ was considered statistically significant.

Abbreviations

PBS, phosphate-buffered saline; LPS, lipopolysaccharide; MCP-1, monocyte chemoattractant protein-1; TNF-α, tumor necrosis factor-α; FSS, fluid shear stress; HP, hydrostatic pressure; TGF-β1, transforming growth factor-β1.

4.3 Results

We could stably apply pulsatile (frequency; 0.5 Hz) FSS with an average magnitude of 0.5 Pa or HP with amplitude of 50 mmHg on cultured macrophages for 30 min without apparent cell detachment (Figure 15A). In the case of FSS experiments, the flow system was adjusted to generate 50 mmHg pressure waves to dissect shear stress-specific effects. On the other hand, the culture medium movement was kept minimal for HP experiments.

30-min FSS significantly decreased the expression of MCP-1, but not TNF-α, in LPS-treated peritoneal macrophages (Figure 15B), whereas application of HP alone for 30 min significantly enhanced both MCP-1 and TNF-α expressions (Figure 15C). Notably, the expressions of other inflammation-related proteins, CD206 (anti-inflammatory) [119] and TGF-β1 (either pro- or anti-inflammatory) [120] were not significantly altered by FSS application. This suggests that the suppressive effect of FSS is fairly specific for MCP-1. In contrast, the increases in MCP-1 and TNF-α expressions and the decrease in CD206 expression after HP application (Figure 15C) indicate that HP has pro-inflammatory properties.

4.4 Discussion

We were unable to reliably apply pulsatile FSS with an average magnitude of ≥1 Pa or HP with a frequency of ≥1 Hz because of technical limitations concerning cell adhesion and precision of pressure control. We cannot thoroughly exclude the possibility that macrophages respond differently to FSS with higher magnitudes. However, anti-inflammatory effects have been reported to be more distinct in FSS with higher magnitudes on endothelial cells [121]. Therefore, intramuscular macrophages *in vivo*, which are expected to be exposed to FSS with ~1 Pa during LCC (Supplementary Table S1), may respond more distinctly than we observed *in vitro* in terms of FSS-induced decrease in MCP-1 expression. All in all, our *in vivo* and *in vitro* data suggest that interstitial fluid flow caused by LCC is at least partially responsible for the LCC-induced decrease of MCP-1 expression in intramuscular macrophages (Figure 8F).

Chapter 5

Conclusion remarks

5.1 Conclusion

Despite accumulating evidence regarding beneficial effects of physical exercise on health, it remains unclear how it modulates bodily functions. In a series of experiments, we have exemplified immobilization-induced muscle atrophy as a physical inactivity-induced disruption of organismal homeostasis. Our findings have clarified the significance of local mechanical stress on cells *in situ*, which appears to be at least partly responsible for positive effects of physical exercise.

The functions of macrophages have been extensively studied, and their importance in the regulation of inflammatory processes has been firmly established. However, their mechanosensing role is very poorly understood or hardly recognized. In this study, we demonstrate that cultured macrophages are sensitive to FSS with an average magnitude of 0.5 Pa (Figure 15B). Together with the resistance of gastrocnemius muscle of clodronate liposome-administered mice to hindlimb immobilization (Figures 9B-9E), mechanosensory function of macrophages recruited from circulating blood appear to be involved in tissue homeostasis. Whereas the decrease in MCP-1 expression in cultured macrophages by FSS relates to anti-inflammation, both pro- and anti-inflammatory effects of cyclical stretching of cultured macrophages have been reported [122, 123]. Such variation might be due to the complexity of cyclical stretching, which is a combination of stretching and relaxation that can affect cellular signaling in opposite directions [124].

Interstitial fluid, which is the most abundant extracellular fluid with 4 times volume as compared to circulating blood [125], is distributed throughout the entire body. Although the importance of interstitium in the regulation of organismal functions is being uncovered [126], interstitial fluid has been recognized to be mainly involved in local delivery of nutrients and removal of metabolic wastes [127]. To date,

mechanical roles of interstitial fluid have not been demonstrated with very few exceptions including that in bone canaliculi which regulates bone homeostasis through FSS on osteocytes [128]. In this study, we show that LCC, which generates intramuscular pressure waves mimicking the condition of mild muscle contraction [129], produces interstitial fluid flow, leading to shear stress exertion on macrophages *in situ*. Still, the majority of cells in parenchymal tissues are exposed to interstitial fluid, and mechanosensing is a universal cellular function [130]. Therefore, it is possible that cells other than macrophages, such as fibroblasts, also contribute to LCC-mediated alleviation of immobilization-induced muscle atrophy. The critical role of interstitial fluid flow as a cause of shear stress on cells *in situ* is compatible with the fact that edema, a condition characterized by local fluid accumulation and likely reduced interstitial fluid flow, is a representative symptom of local inflammation.

Bodily motions, with no exception, produce changes of stress distribution, i.e. local pressure changes, which generate interstitial fluid flow. Animals are defined so because of their ability to generate bodily motions voluntarily. Currently, the anti-inflammatory effects of FSS have been mainly shown for vascular endothelial cells with particular reference to its regularity and magnitude [131]. Our quantitative analysis of the interstitial fluid dynamics combined with our simulative calculation indicates that intramuscular interstitial cells are subjected to FSS with average magnitude of ~1 Pa, which coincides with that exerted on vascular endothelial cells [132] or osteocytes [133]. Therefore, we speculate that FSS of this range of magnitudes produced by bodily motions may be universally involved in organismal homeostasis.

Meanwhile, massage is defined as “a mechanical manipulation of body tissues with rhythmical pressure and stroking for the purpose of promoting health and well-being”

[61]. It is perhaps unanimously agreed that massage relieves local pain/discomfort or even general unpleasantness/revolt. According to the American Massage Therapy Association, massage alleviates local soreness, headache, depression, and sleep disturbance, thereby improving quality of life (http://www.AMTA./org). However, there is a conflict concerning scientific evidence related to massage effects [134]. The anti-inflammatory effects of massage on skeletal muscles have not been demonstrated with mechanistic insights, including those into the effector cells for massage. We have demonstrated LCC, a massage-like intervention, evokes interstitial flow, possibly leading to shear stress exertion on macrophages *in situ*. Our findings suggest the common mechanism behind the disuse muscle atrophy as well as the beneficial effects of physical exercise and massage (Figure 16). This study may provide a cue to deciphering the mechanism of massage as a pain- and inflammation-relieving procedure and harnessing its effects towards a development of novel therapy.

5.2 Potential of mechanical stress

Mechanical stress influences every area of biology, from early developmental process to adult physiology and pathology. In the adult organism, several physiological processes are dependent on mechanical stress sensing, including the senses of hearing and touch. There is also a dark side by pathological forces, such as tumor metastasis and atherosclerosis [135, 136]. As existing at the blood vessel interface, endothelial cells are continually exposed to blood flow (i.e. mechanical stress). Therefore, research on mechanical stress has progressed in terms of endothelial cells.

Endothelial cells own many mechanosensors on the basal surfaces. These potential mechanosensors sense blood flow, and convert physical strength into biochemical signals [137]. The stress patterns produced by blood flow differ based on vessel

geometry. These patterns range from uniform flow to nonuniform perturbed flow. Although endothelial cells sense and differentially react to flow patterns specific to their microenvironment, little is known about the underlying mechanisms of endothelial mechanosensing. On the other hand, despite exposure to mechanical stress resulting from their shape changes due to muscle contraction, there have been relatively few studies on the underlying mechanisms of skeletal muscle mechanosensing.

As for immune system and macrophages, much less work has been done on the biological effects of mechanical stress. The current studies propose a possibility that monocytes/macrophages-included mechanosignaling affects tumor development. Mechanosensing is the process, in which altered physical stimuli of the extracellular matrix are transduced into biochemical signals to direct cellular actions [138]. Mechanosensing pathways are activated by stimuli to adhesion receptors (e.g. integrins and CD44), leading to changes of cytoskeletal tension and downstream signaling, ultimately controlling many processes for induction of tumor onset and progression [139-141]. However, the role of macrophage has not been made it clear. Notably, adhesion receptors of macrophages can also interact with receptors related to inflammation by sharing similar downstream signaling. Thus, altered extracellular matrix characteristics can additionally modulate immune cell actions indirectly.

Very few attempts have been made at clarifying the ‘factors’ of aerobic exercise. In this thesis, we proposed that the factors were the biological benefits of mechanical stress brought by interstitial fluid flow. These findings clarified the significance of local mechanical stress on cells *in situ*, which appears to be at least partly responsible for positive effects of physical exercise. Understanding the mechanisms, by which mechanosensors sense and react to mechanical stress, provides the scientific evidence

for the benefits of moderate exercise, and open a new path to develop a novel therapeutic strategy or an alternative intervention.

Chapter 6

Figures and Table

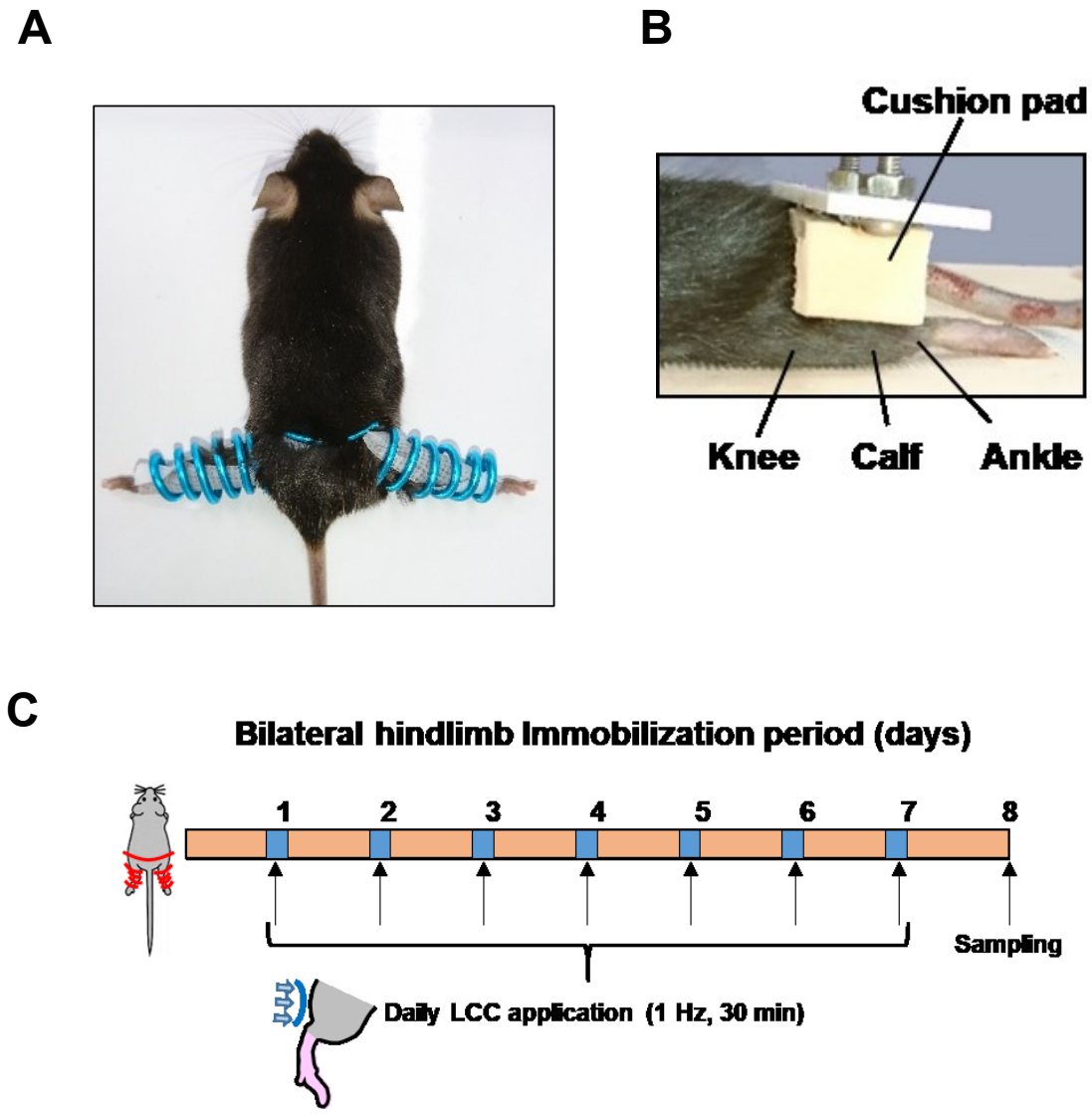

Figure 1. (A) Bilateral hindlimb immobilization. Deformable metal wire was adjusted to immobilize bilateral hindlimbs of mice. (B) Experimental set-up for LCC. (C) LCC (1 Hz, 30 min) was applied daily to one of the hindlimbs during immobilization for 8 days.

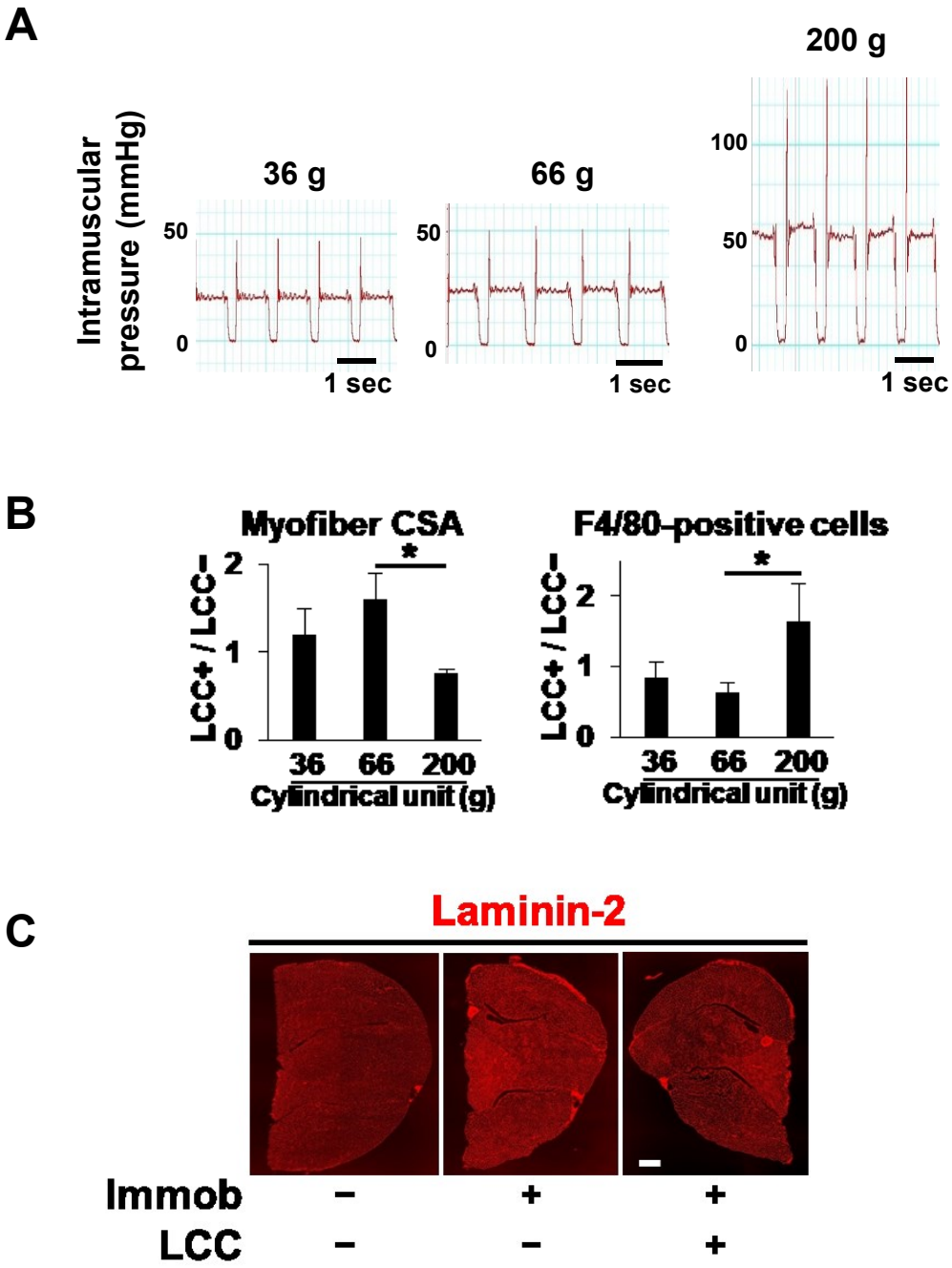

Figure 2. (A) Intramuscular pressure waves during LCC. Scale bar, 1 sec. (B) Comparison of the effects of LCC application to immobilized hindlimbs with 36-g, 66-g and 200-g cylindrical units. CSA of gastrocnemius myofibers (left) and F4/80-positive cells (right) of LCC-applied calf were quantified as relative values to those of the control hindlimb, which was not exposed to LCC, in each mouse. Data are presented as means ± S.D. *, $P < 0.05$, one-way ANOVA with post hoc Bonferroni test (n = 4 mice for each group). (C) No apparent injury after LCC application. Representative anti-laminin-2 immunostaining images of triceps surae muscles of unimmobilized (left) and immobilized hindlimbs without (center) or with (right) 7 times daily LCC application. The center and right micrographs are from the same mouse. Scale bar, 500 µm.

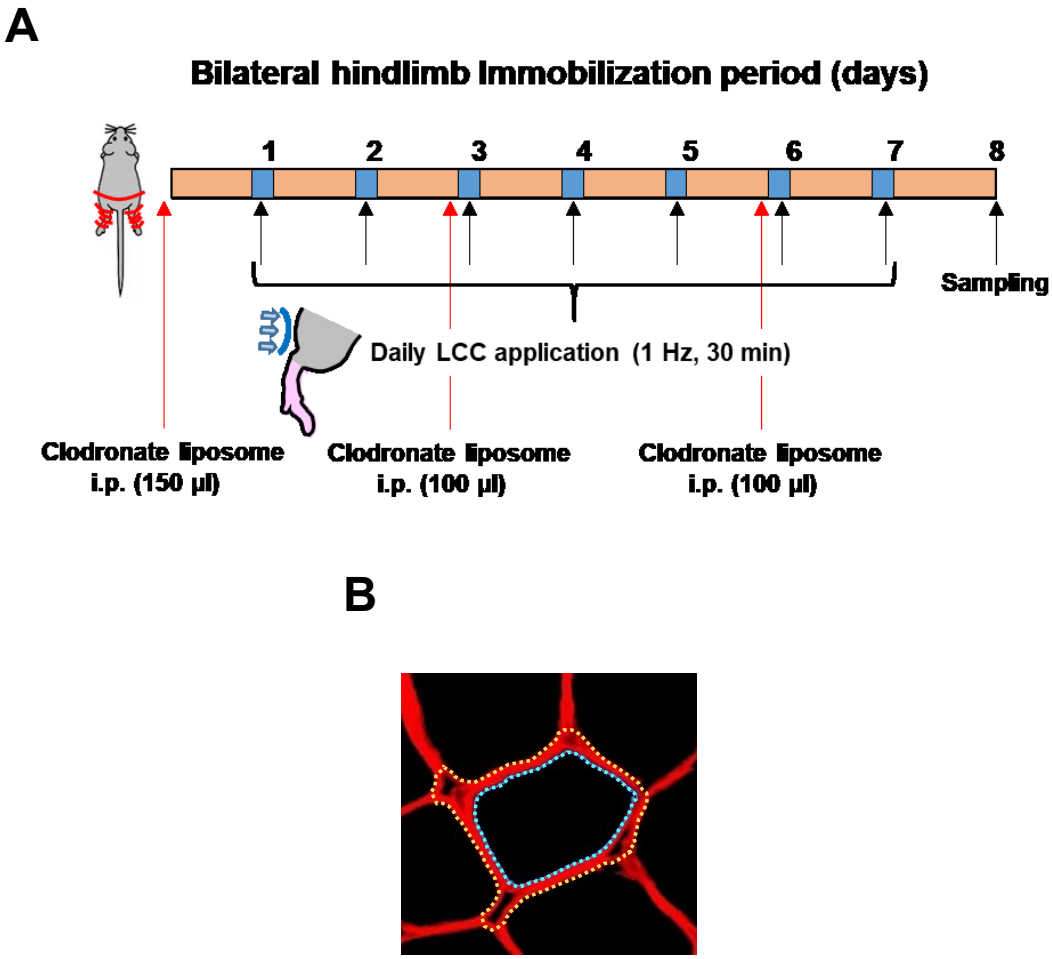

Figure 3. (A) Dose and time points of clodronate liposome administration. (B) Schematic representation of the definition as to the CSA and the interstitial space. The 'internal' and 'external' margins of basement membrane surrounding a gastrocnemius myofiber, which were visualized by anti-laminin-2 immunostaining, are traced with cyan and yellow dot lines, respectively.

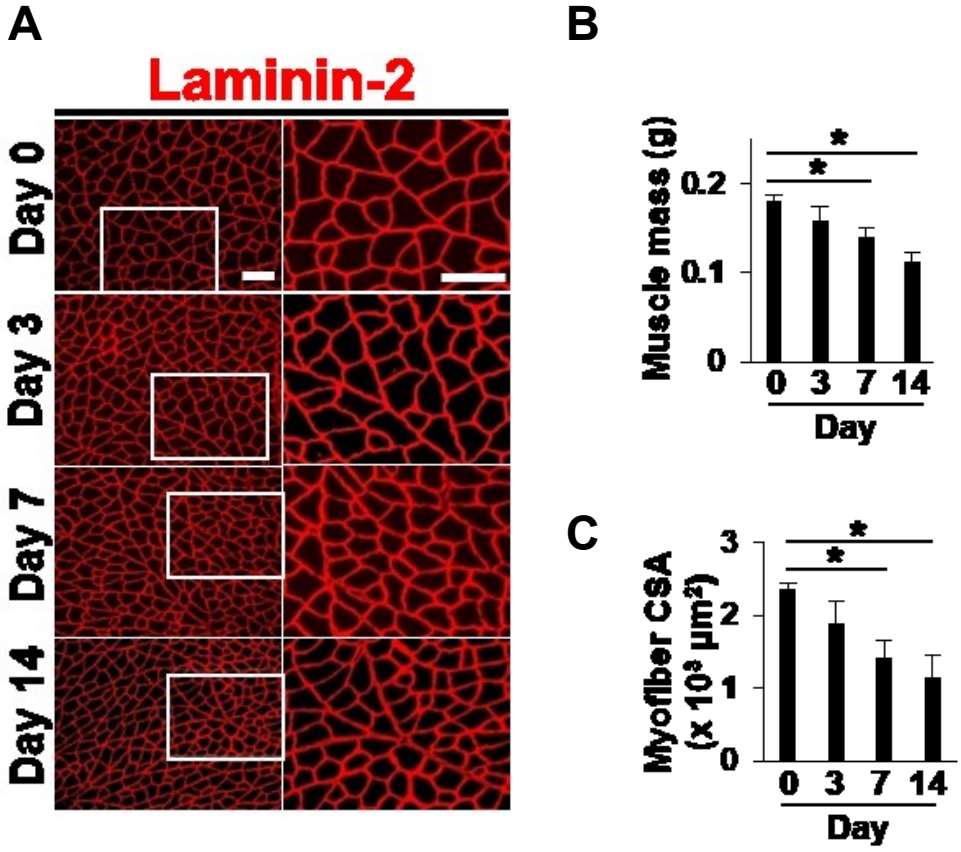

Figure 4. (A) Cross-sectional micrographic images of anti-laminin-2 immunofluorescence staining of gastrocnemius muscles. High magnification images (right) refer to the areas indicated by rectangles in low magnification images (left). Scale bars, 100 μm. (B) Triceps surae muscle mass. (C) CSA of gastrocnemius myofibers. decreased with the period of hindlimb immobilization. To quantify CSA, 100 myofibers were randomly chosen. Data are presented as means ± S.D. *, P < 0.05, one-way ANOVA with post hoc Bonferroni test (n = 3 mice for each group).

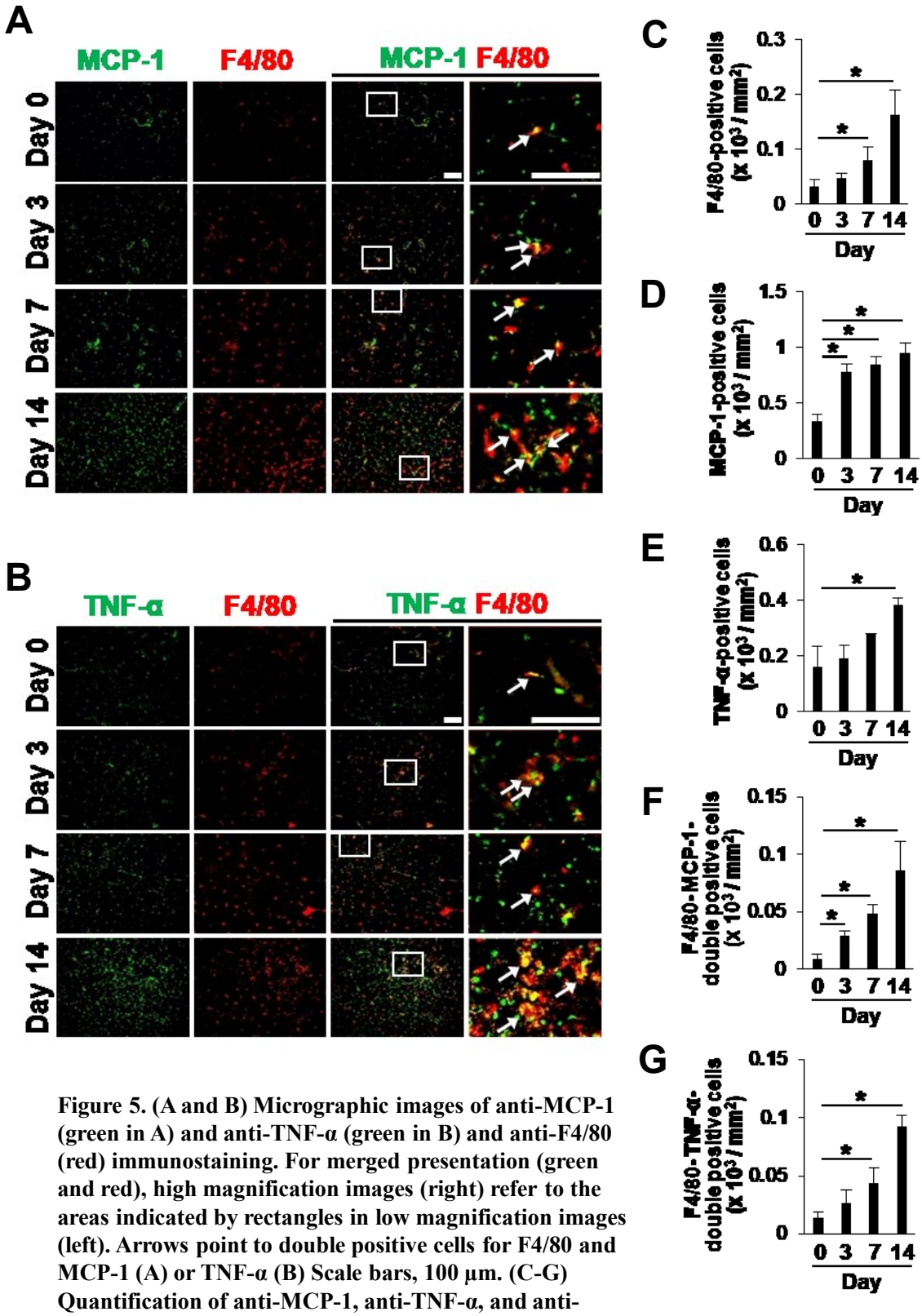

Figure 5. (A and B) Micrographic images of anti-MCP-1 (green in A) and anti-TNF-α (green in B) and anti-F4/80 (red) immunostaining. For merged presentation (green and red), high magnification images (right) refer to the areas indicated by rectangles in low magnification images (left). Arrows point to double positive cells for F4/80 and MCP-1 (A) or TNF-α (B) Scale bars, 100 μm. (C-G) Quantification of anti-MCP-1, anti-TNF-α, and anti-F4/80 immunostaining. Data are presented as means ± S.D. *, $P < 0.05$, one-way ANOVA with post hoc Bonferroni test (n = 3 mice for each group).

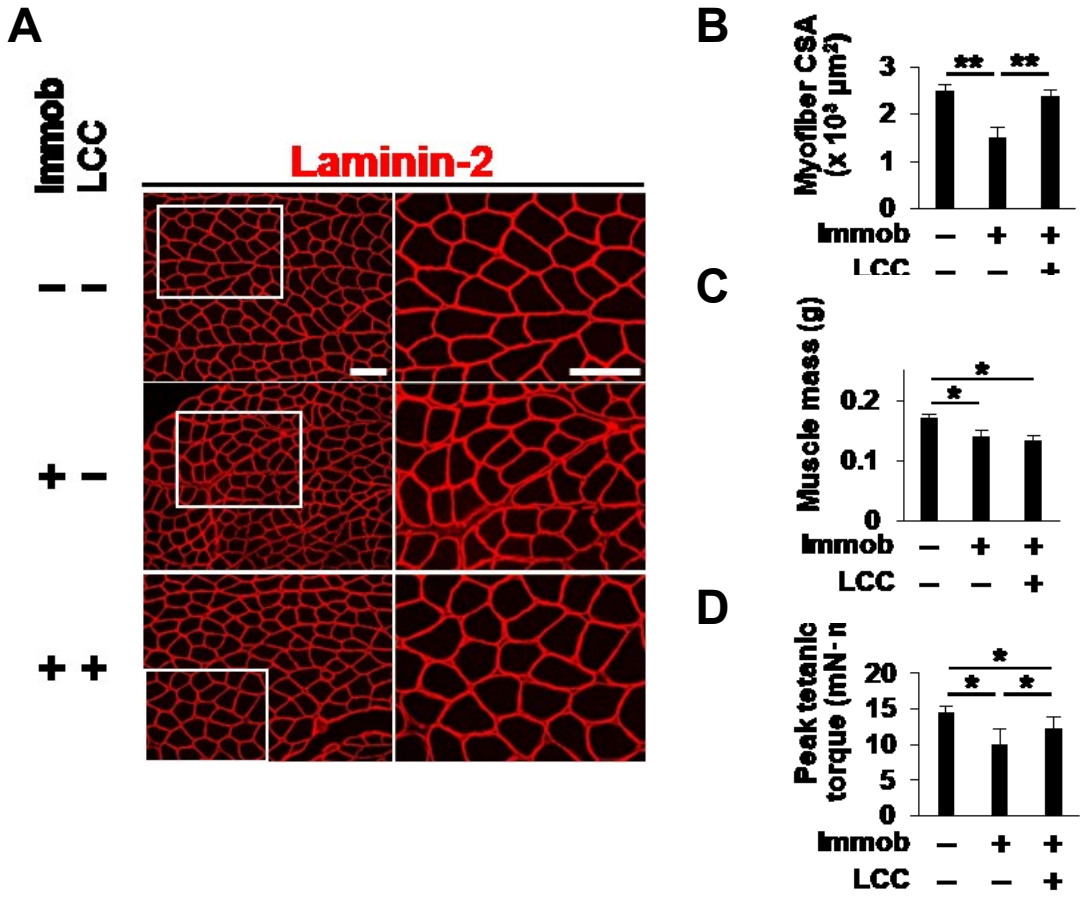

Figure 6. (A) Cross-sectional micrographic images of anti-laminin-2 immunofluorescence staining of gastrocnemius muscles. High magnification images (right) refer to the areas indicated by rectangles in low magnification images (left). Scale bars, 100 μm. (B) CSA of gastrocnemius myofibers. (C)triceps surae muscle mass. (B)(C)Data are presented as means ± S.D. *, P < 0.05; **, P < 0.01, one-way ANOVA with post hoc Bonferroni test (n = 6 mice for each group). (D) Decrease in contracting force of triceps surae muscles after immobilization and its partial restoration by LCC. Data are presented as means ± S.D. *, P < 0.05, paired Student's t test (n = 4 mice for control, n = 5 mice for immobilization group).

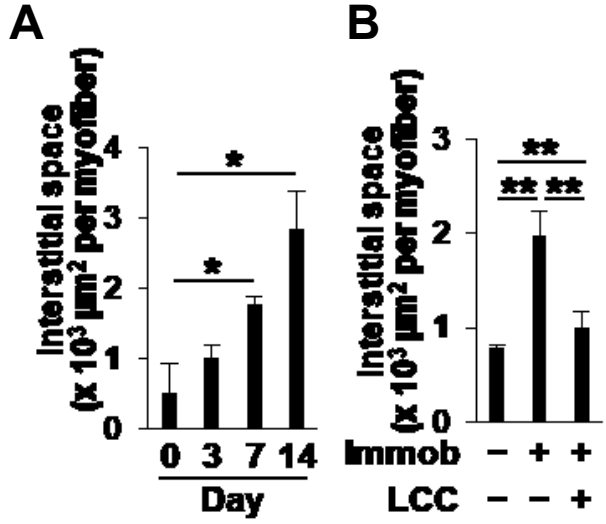

Figure 7. (A) Interstitial space in muscle tissues increased with the period of immobilization. (B) LCC alleviated the immobilization-induced increase of interstitial space in muscle tissues. Data are presented as means ± S.D. *, P < 0.05; **, P < 0.01, one-way ANOVA with post hoc Bonferroni test. (A)n=3 mice for each group. (B) n = 4 mice for control, n = 5 mice for immobilization group.

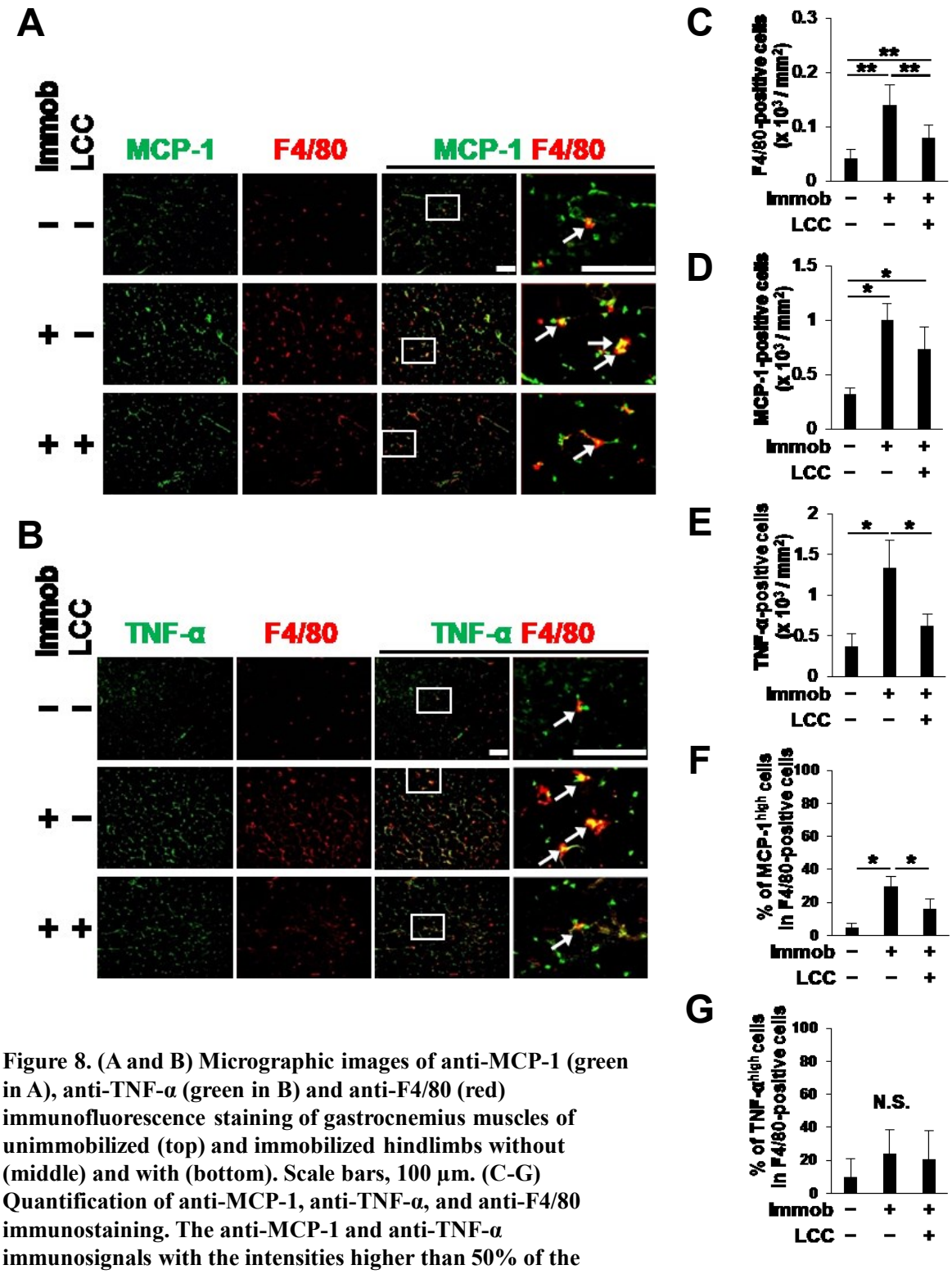

Figure 8. (A and B) Micrographic images of anti-MCP-1 (green in A), anti-TNF-α (green in B) and anti-F4/80 (red) immunofluorescence staining of gastrocnemius muscles of unimmobilized (top) and immobilized hindlimbs without (middle) and with (bottom). Scale bars, 100 µm. (C-G) Quantification of anti-MCP-1, anti-TNF-α, and anti-F4/80 immunostaining. The anti-MCP-1 and anti-TNF-α immunosignals with the intensities higher than 50% of the highest ones in the respective staining were defined as MCP-1high (F) and TNF-αhigh (G), respectively. Data are presented as means ± S.D. N.S., not significant, *, P < 0.05; **, P < 0.01, one-way ANOVA with post hoc Bonferroni test (n = 6 mice for each group).

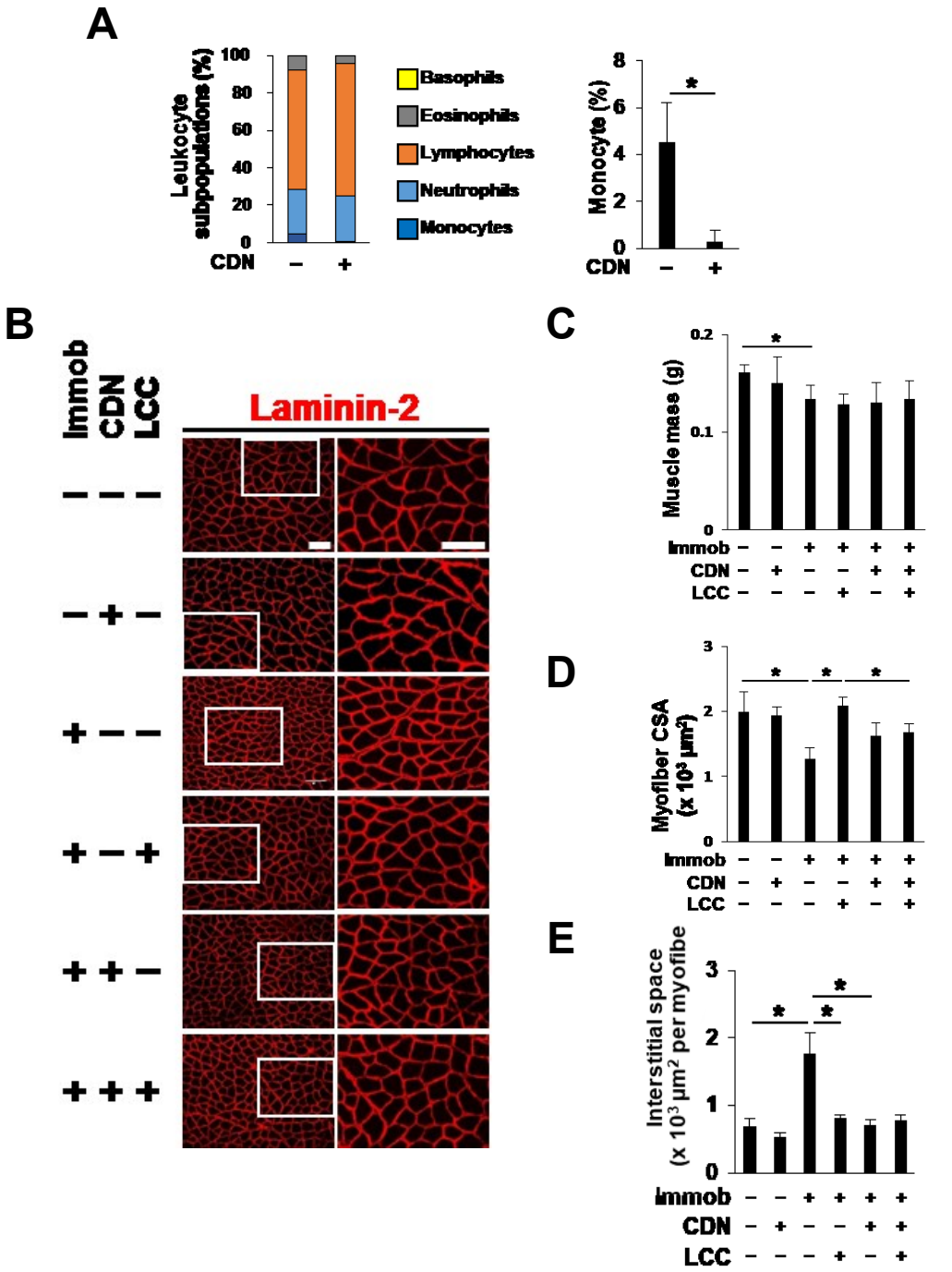

Figure 9. (A) Clodronate liposome administration depleted monocytes in circulating blood. Eighteen hours after intraperitoneal injection of clodronate or control liposomes (200 µl), 12-week-old male mice were subjected to blood sampling for differential white blood cell count. Data are presented as means ± S.D. *, P < 0.05, paired Student's t test (n = 4 mice for each group). (B) Cross-sectional micrographic images of anti-laminin-2 immunofluorescence staining of gastrocnemius muscles. High magnification images (right) refer to the areas indicated by rectangles in low magnification images (left). Scale bars, 100 µm. (C)Triceps surae muscle mass. (D) CSA of gastrocnemius myofibers. (E) Interstitial space. Data are presented as means ± S.D. *, P < 0.05, unpaired Student's t test (n = 5 mice for each group of control liposome administration; n = 6 mice for each group of clodronate liposome administration).

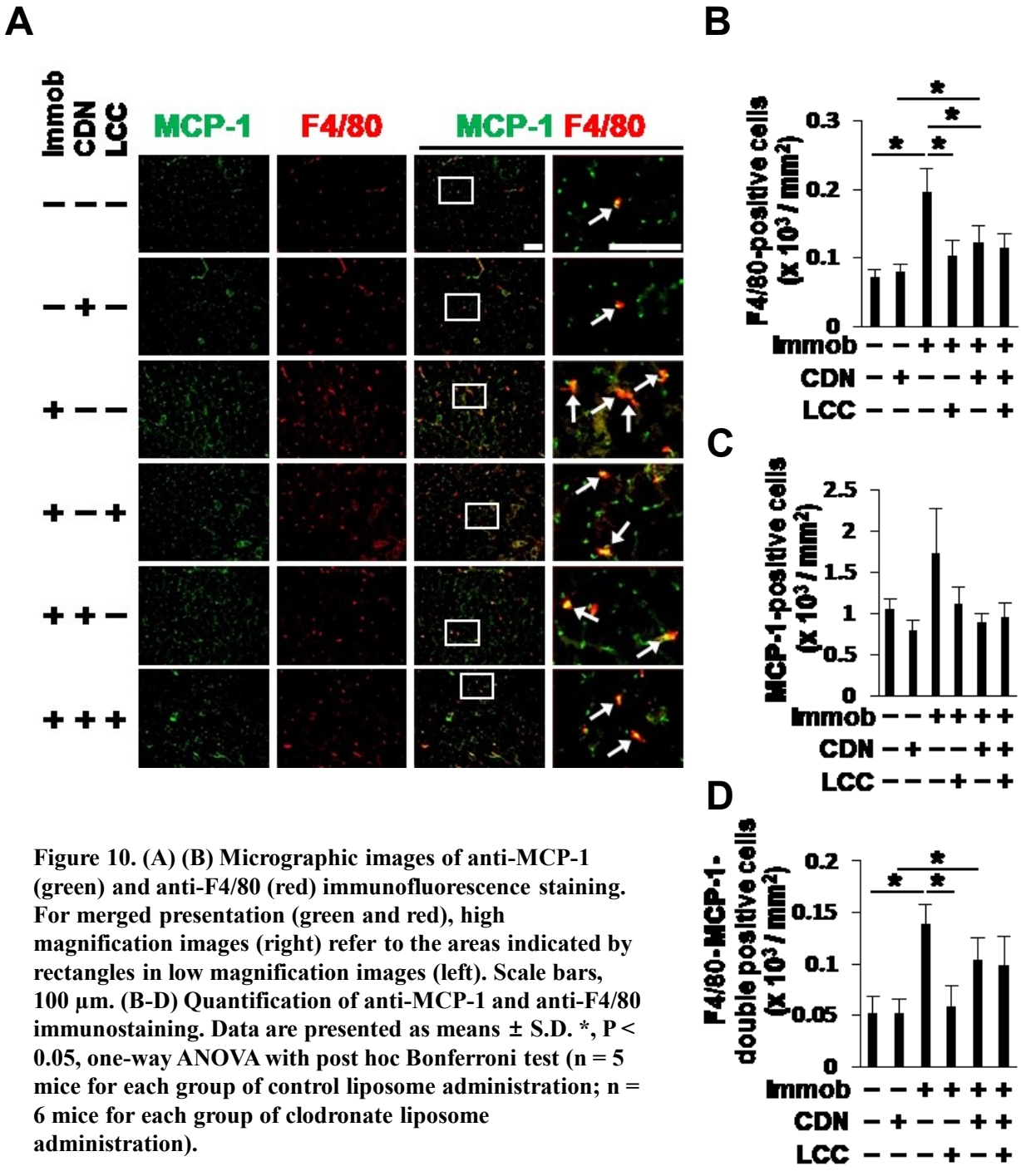

Figure 10. (A) (B) Micrographic images of anti-MCP-1 (green) and anti-F4/80 (red) immunofluorescence staining. For merged presentation (green and red), high magnification images (right) refer to the areas indicated by rectangles in low magnification images (left). Scale bars, 100 µm. (B-D) Quantification of anti-MCP-1 and anti-F4/80 immunostaining. Data are presented as means ± S.D. *, P < 0.05, one-way ANOVA with post hoc Bonferroni test (n = 5 mice for each group of control liposome administration; n = 6 mice for each group of clodronate liposome administration).

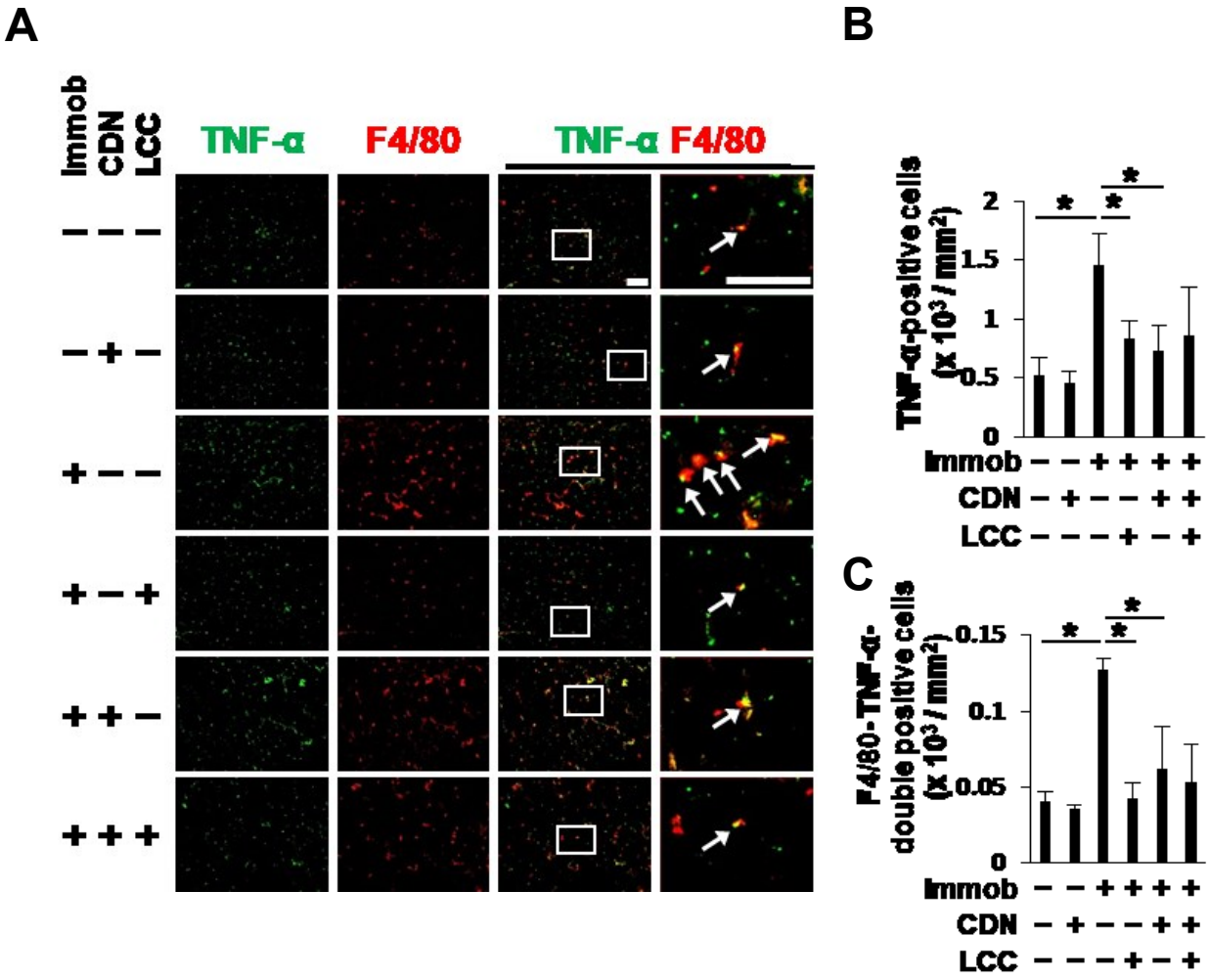

Figure 11. (A) Micrographic images of anti-TNF-α (green) and anti-F4/80 (red) immunofluorescence staining. For merged presentation (green and red), high magnification images (right) refer to the areas indicated by rectangles in low magnification images (left). Scale bars, 100 μm. (B)(C) Quantification of anti-TNF-α and anti-F4/80 immunostaining. Data are presented as means ± S.D. *, P < 0.05, one-way ANOVA with post hoc Bonferroni test (n = 5 mice for each group of control liposome administration; n = 6 mice for each group of clodronate liposome administration).

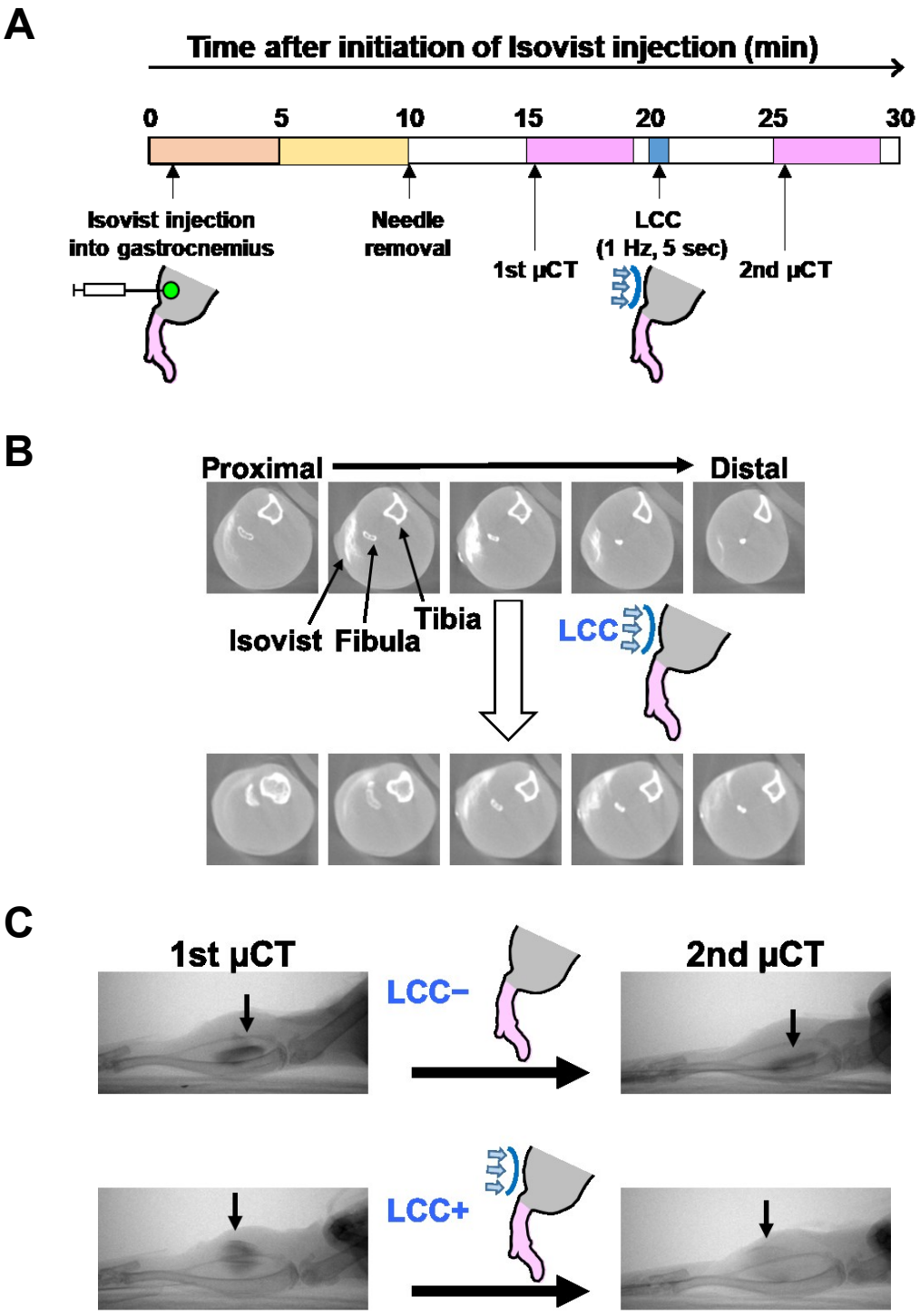

Figure 12. (A) LCC was applied for 5 sec (6 strokes) between two serial µCT scans. (B) Axial-view µCT images of a contrast medium (Isovist)-injected mouse calf before (top panel) and after (bottom panel) LCC. After injecting 3 µl of Isovist into the mid-belly of gastrocnemius muscle, two consecutive µCT scanning was conducted interposing 5-sec LCC application. (C) Representative X-ray radiographs imaging contrast medium (Isovist) injected into gastrocnemius muscle bellies of mice, either exposed or left unexposed to LCC on their calves for 5 sec. LCC was applied between the 1st and 2nd imaging. Arrows point to Isovist clusters.

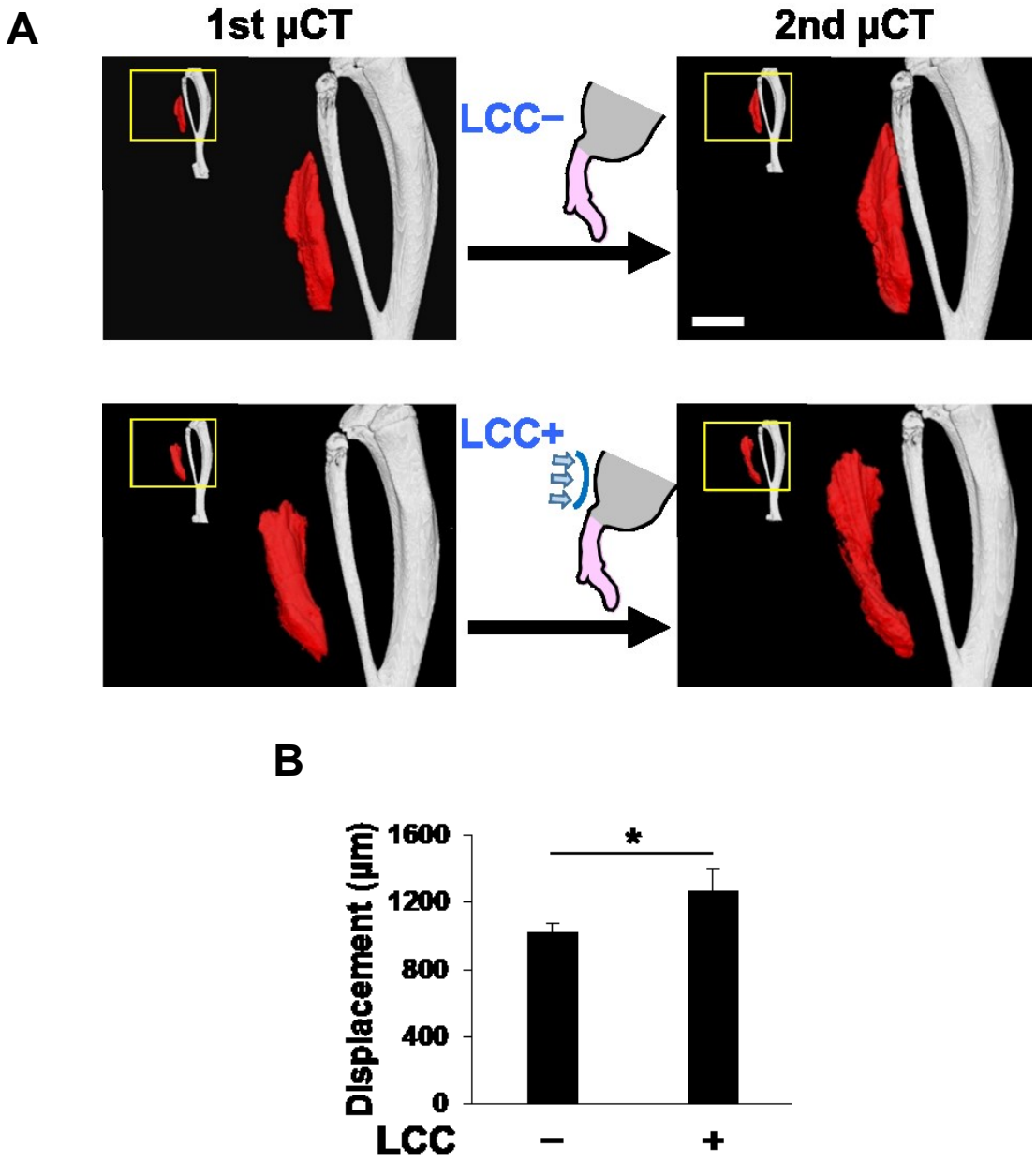

Figure 13. (A) Simulative representation of spreading of Isovist injected into gastrocnemius muscle bellies of mice, either exposed (bottom) or left unexposed (top) to LCC on their calves for 5 sec. Isovist spreading is indicated as red clusters. Scale bar, 2 mm. (B) LCC increased Isovist movement. The movement of Isovist cluster defined as in (A) was quantified by measuring the displacement of its proximal end between the first and the second μCT images. Data are presented as means ± S.D. *, $P < 0.05$, paired Student's t test (n = 4 legs for each group).

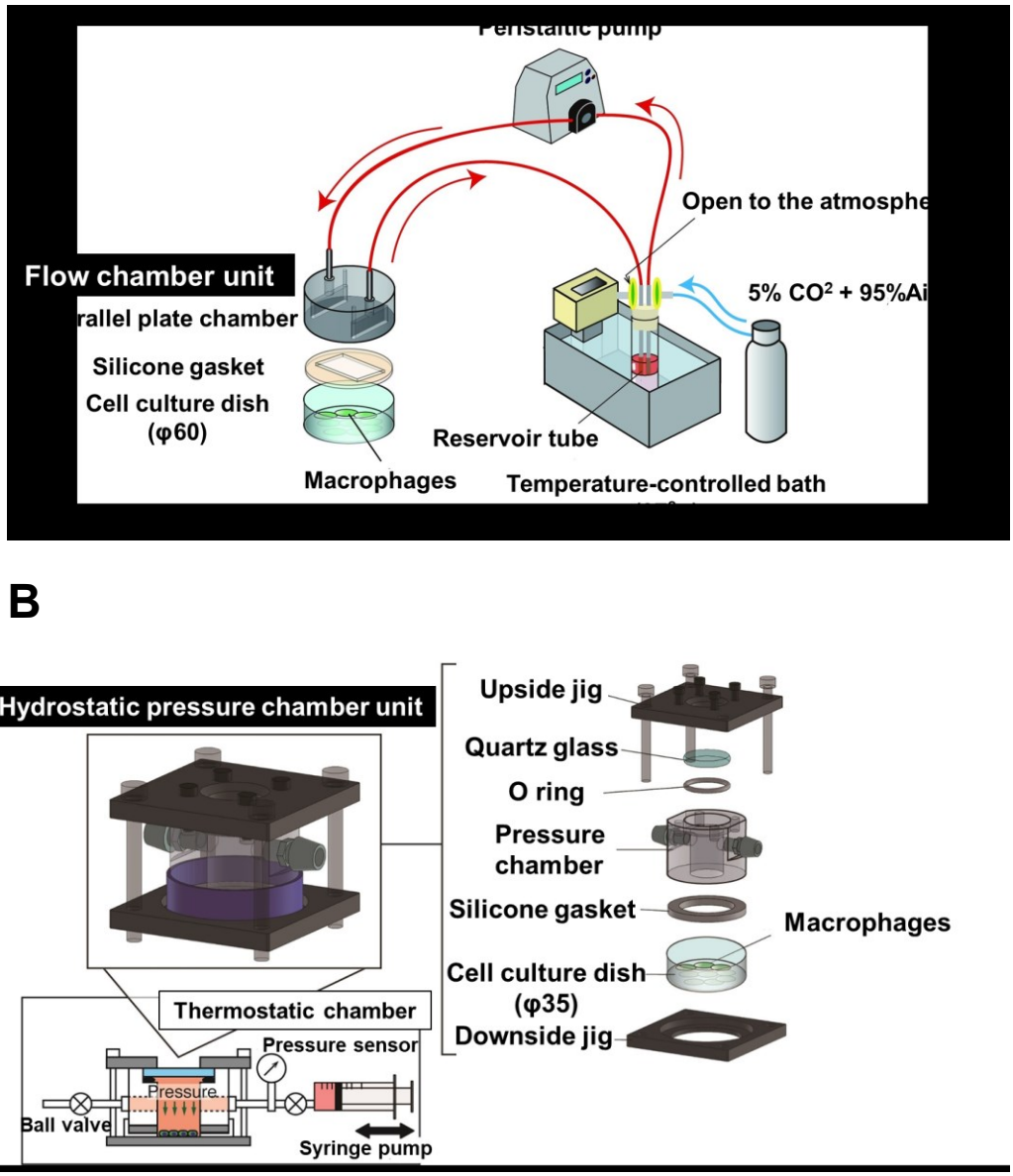

Figure 14. (A and B) Schematic representations of custom-made systems for FSS (A) and HP (B).

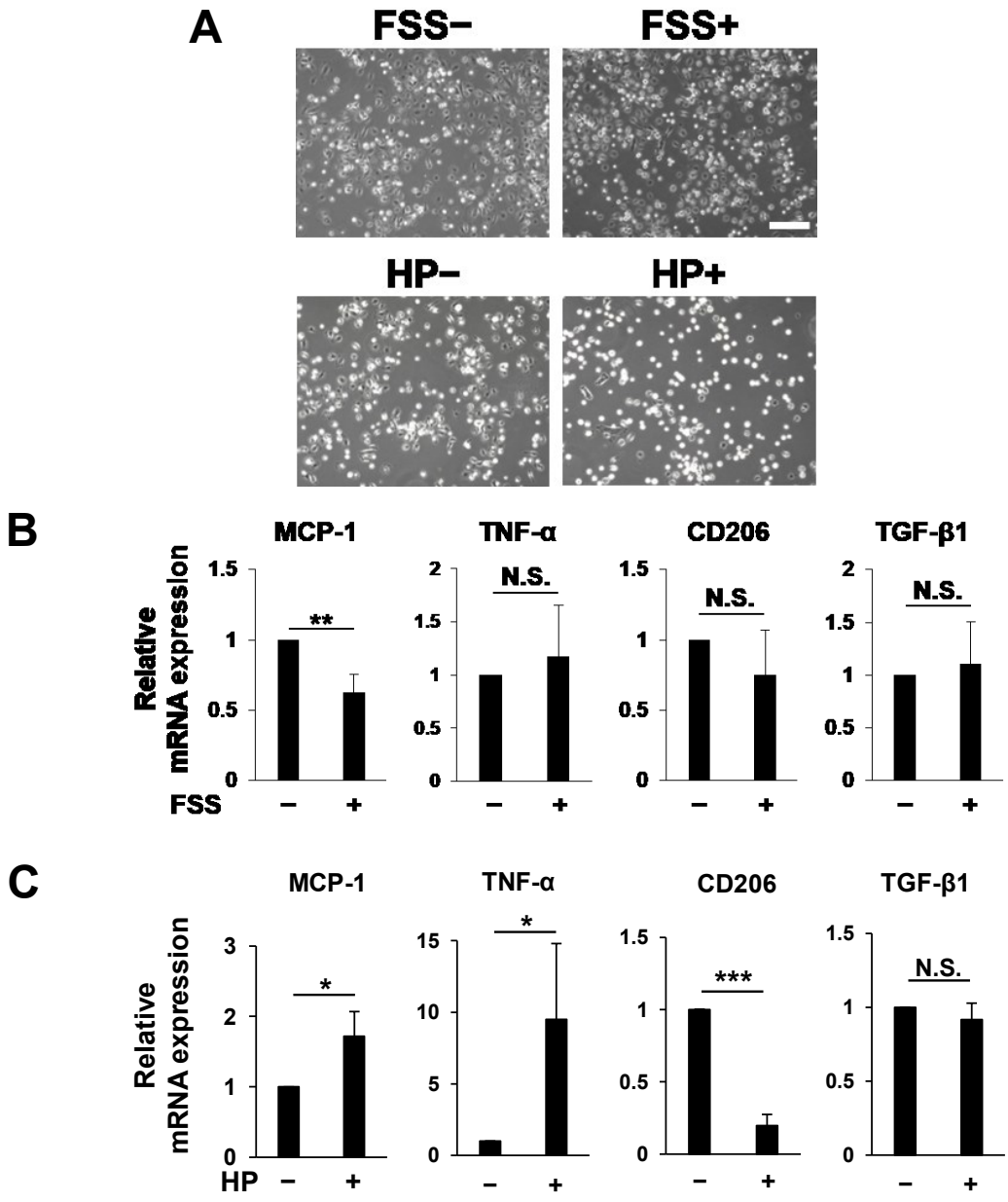

Figure 15. (A) Representative micrographic images of mouse peritoneal macrophages pre-treated with LPS before (top left) or after (top right) pulsatile FSS application (frequency; 0.5 Hz, average magnitude; 0.5 Pa, zero-to-peak mode) and before (bottom left) or after (bottom right) pulsatile HP application (frequency; 0.5 Hz, amplitude; 50 mmHg) for 30 min. Scale bar, 200 µm. (B) LPS-pretreated peritoneal macrophages were either exposed or left unexposed to pulsatile FSS for 30 min. mRNA expression levels were normalized against GAPDH, and scaled with the control sample (FSS-) set at 1 in each experiment. Data are presented as means ± S.D. N.S., not significant, **, P < 0.01, paired Student's t test (n = 5). (C) LPS-pretreated peritoneal macrophages were either exposed or left unexposed to pulsatile HP for 30 min. mRNA expression levels were normalized against GAPDH, and scaled with the control sample (HP-) set at 1 in each experiment. Data are presented as means ± S.D. N.S., not significant, *, P < 0.05, ***, P < 0.001, paired Student's t test (n = 5).

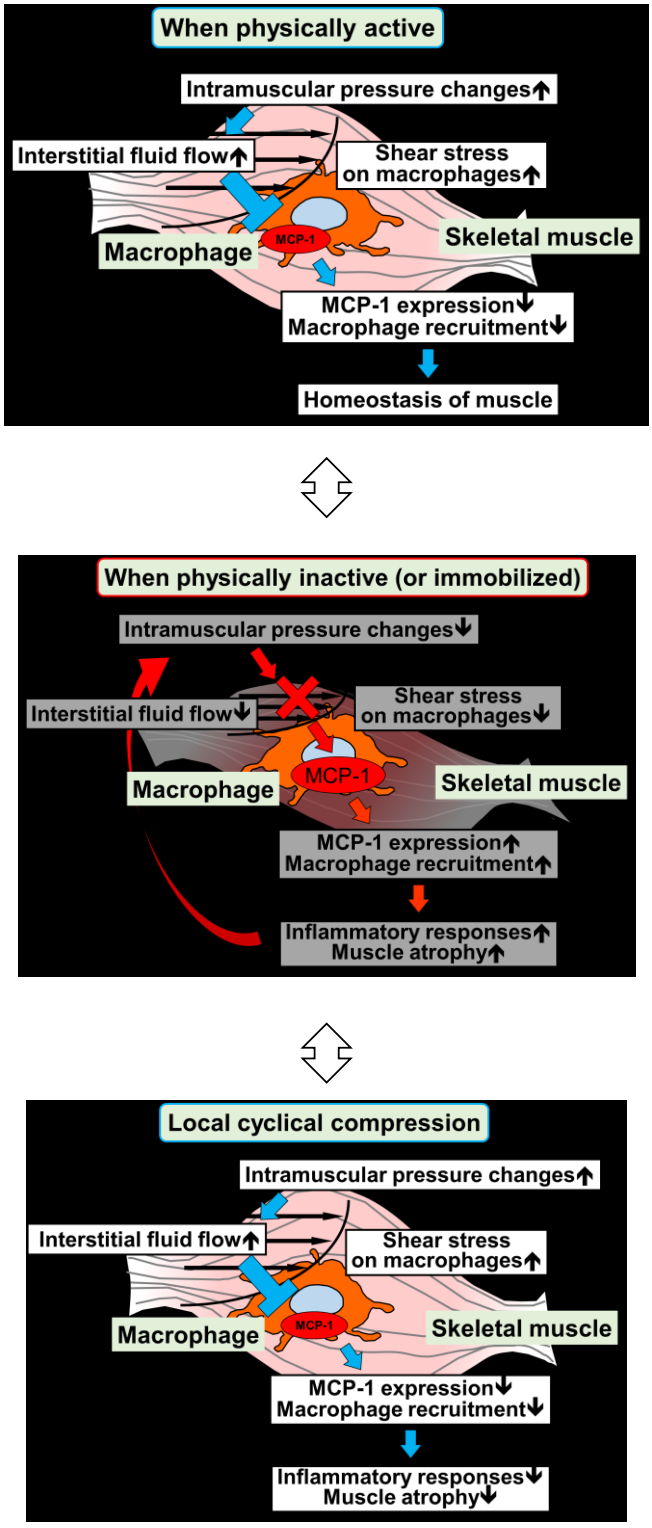

Figure 16. Schematic representation of the molecular mechanism behind the physical inactivity-induced atrophy of muscle as well as its restoration by LCC, involving the mechanosensory function of macrophages in situ

A

Property	Value
Pressure (ΔP; Pa)	3657.29
Viscosity (μ; mPa·s)	1.20 - 1.90*
Distance of movement (Δd; μm)	238.59
Velocity of interstitial fluid flow (u_w; μm/s)	47.72
Shear stress (Pa)	0.94 - 1.18

B

Fluid shear stress (τ) at the cell surface:

$$\tau = \mu u_w / \sqrt{K_p}$$
$$K_p = \mu u_w \Delta d / \Delta P$$

, where K_p is the Darcy permeability of muscle tissue.

When the values listed in A are introduced in these equations, the magnitude of fluid shear stress is estimated as 0.94 - 1.18 Pa.

Table (A) Values referenced for simulative calculation of the magnitude of FSS that LCC generated in the gastrocnemius muscles. All referenced values except viscosity (marked by an asterisk) were drawn from analyses with intramuscular pressure measurement (Figure 2A) and Isovist-enhanced μCT scanning (Figure 13). The property of interstitial fluid viscosity was referenced from previous studies [110,111]. (B) Calculation of the magnitude of LCC-generated fluid shear stress. Fluid shear stress (τ) at the cell surface can be calculated as reported previously [142].

Chapter 7

References

1 Ogawa, T., Furochi, H., Mameoka, M., Hirasaka, K., Onishi, Y., Suzue, N., Oarada, M., Akamatsu, M., Akima, H., Fukunaga, T., Kishi, K., Yasui, N., Ishidoh, K., Fukuoka, H. and Nikawa, T. (2006) Ubiquitin ligase gene expression in healthy volunteers with 20-day bedrest. Muscle Nerve. **34**, 463-469

2 Haus, J. M., Carrithers, J. A., Carroll, C. C., Tesch, P. A. and Trappe, T. A. (2007) Contractile and connective tissue protein content of human skeletal muscle: effects of 35 and 90 days of simulated microgravity and exercise countermeasures. American Journal of Physiology-Regulatory, Integrative and Comparative Physiology. **293**, R1722-R1727

3 LeBlanc, A., Rowe, R., Schneider, V., Evans, H. and Hedrick, T. (1995) Regional muscle loss after short duration spaceflight. Aviat. Space Environ. Med. **66**, 1151-1154

4 Hunter, R. B., Stevenson, E. J., Koncarevic, A., Mitchell-Felton, H., Essig, D. A. and Kandarian, S. C. (2002) Activation of an alternative NF-κB pathway in skeletal muscle during disuse atrophy. The FASEB Journal. **16**, 529-538

5 Senf, S. M., Dodd, S. L., McClung, J. M. and Judge, A. R. (2008) Hsp70 overexpression inhibits NF-κB and Foxo3a transcriptional activities and prevents skeletal muscle atrophy. The FASEB Journal. **22**, 3836-3845

6 Babij, P. and Booth, F. W. (1988) Alpha-actin and cytochrome c mRNAs in atrophied adult rat skeletal muscle. American Journal of Physiology-Cell Physiology. **254**, C651-C656

7 Ventadour, S. and Attaix, D. (2006) Mechanisms of skeletal muscle atrophy. Curr. Opin. Rheumatol. **18**, 631-635

8 Ikemoto, M., Nikawa, T., Takeda, S. I., Watanabe, C., Kitano, T., Baldwin, K. M., Izumi, R., Nonaka, I., Towatari, T., Teshima, S., Rokutan, K. and Kishi, K. (2001) Space shuttle flight (STS-90) enhances degradation of rat myosin heavy chain in association with activation of ubiquitin–proteasome pathway. The FASEB Journal. **15**, 1279-1281

9 Lecker, S. H., Solomon, V., Mitch, W. E. and Goldberg, A. L. (1999) Muscle protein breakdown and the critical role of the ubiquitin-proteasome pathway in normal and disease states. The Journal of Nutrition. **129**, 227S-237S

10 Kandarian, S. C. and Stevenson, E. J. (2002) Molecular events in skeletal muscle during disuse atrophy. Exerc. Sport Sci. Rev. **30**, 111-116

11 Reid, M. B. (2005) Response of the ubiquitin-proteasome pathway to changes in muscle activity. American Journal of Physiology-Regulatory, Integrative and Comparative Physiology. **288**, R1423-R1431

12 Bodine, S. C., Latres, E., Baumhueter, S., Lai, V. K.-M., Nunez, L., Clarke, B. A., Poueymirou, W. T., Panaro, F. J., Na, E., Dharmarajan, K., Pan, Z.-Q., Valenzuela, D. M., DeChiara, T. M., Stitt, T. N., Yancopoulos, G. D. and Glass, D. J. (2001) Identification of ubiquitin ligases required for skeletal muscle atrophy. Science. **294**, 1704-1708

13 Medina, R., Wing, S. S. and Goldberg, A. L. (1995) Increase in levels of polyubiquitin and proteasome mRNA in skeletal muscle during starvation and denervation atrophy. Biochem. J. **307**, 631-637

14 Medina, R., Wing, S. S., Haas, A. and Goldberg, A. L. (1991) Activation of the ubiquitin-ATP-dependent proteolytic system in skeletal muscle during fasting and denervation atrophy. Biomed. Biochim. Acta. **50**, 347-356

15 Jones, S. W., Hill, R. J., Krasney, P. A., O'Conner, B., Peirce, N. and Greenhaff, P. L. (2004) Disuse atrophy and exercise rehabilitation in humans profoundly affects the expression of genes associated with the regulation of skeletal muscle mass. The FASEB Journal. **18**, 1025-1027

16 Ikemoto, M., Nikawa, T., Kano, M., Hirasaka, K., Kitano, T., Watanabe, C., Tanaka, R., Yamamoto, T., Kamada, M. and Kishi, K. (2002) Cysteine Supplementation Prevents Unweighting-Induced Ubiquitination in Association with Redox Regulation in Rat Skeletal Muscle. In Biol. Chem. **383**(3-4):715-21

17 Coffey, V. G., Shield, A., Canny, B. J., Carey, K. A., Cameron-Smith, D. and Hawley, J. A. (2006) Interaction of contractile activity and training history on mRNA abundance in skeletal muscle from trained athletes. American Journal of Physiology-Endocrinology and Metabolism. **290**, E849-E855

18 Louis, E., Raue, U., Yang, Y., Jemiolo, B. and Trappe, S. (2007) Time course of proteolytic, cytokine, and myostatin gene expression after acute exercise in human skeletal muscle. Journal of Applied Physiology. **103**, 1744-1751

19 Phillips, S. M., Tipton, K. D., Aarsland, A., Wolf, S. E. and Wolfe, R. R. (1997) Mixed muscle protein synthesis and breakdown after resistance exercise in humans. American Journal of Physiology-Endocrinology and Metabolism. **273**, E99-E107
20 Abu Hatoum, O., Gross-Mesilaty, S., Breitschopf, K., Hoffman, A., Gonen, H., Ciechanover, A. and Bengal, E. (1998) Degradation of Myogenic Transcription Factor MyoD by the Ubiquitin Pathway In Vivo and In Vitro: Regulation by Specific DNA Binding. Mol. Cell. Biol. **18**, 5670-5677
21 Li, Y.-P. and Reid, M. B. (2000) NF-κB mediates the protein loss induced by TNF-α in differentiated skeletal muscle myotubes. American Journal of Physiology-Regulatory, Integrative and Comparative Physiology. **279**, R1165-R1170
22 Lockhart, N. C. and Brooks, S. V. (2008) Neutrophil accumulation following passive stretches contributes to adaptations that reduce contraction-induced skeletal muscle injury in mice. J Appl Physiol (1985). **104**, 1109-1115
23 Pizza, F. X., Peterson, J. M., Baas, J. H. and Koh, T. J. (2005) Neutrophils contribute to muscle injury and impair its resolution after lengthening contractions in mice. J. Physiol. **562**, 899-913
24 Deng, B., Wehling-Henricks, M., Villalta, S. A., Wang, Y. and Tidball, J. G. (2012) IL-10 triggers changes in macrophage phenotype that promote muscle growth and regeneration. J Immunol. **189**, 3669-3680
25 Serhan, C. N. and Savill, J. (2005) Resolution of inflammation: the beginning programs the end. Nat. Immunol. **6**, 1191
26 Manabe, I. (2011) Chronic inflammation links cardiovascular, metabolic and renal diseases. Circulation journal : official journal of the Japanese Circulation Society. **75**, 2739-2748
27 Elliott, M. R. and Ravichandran, K. S. (2010) Clearance of apoptotic cells: implications in health and disease. J. Cell Biol. **189**, 1059-1070
28 Li, Y.-P., Lecker, S. H., Chen, Y., Waddell, I. D., Goldberg, A. L. and Reid, M. B. (2003) TNF-α increases ubiquitin-conjugating activity in skeletal muscle by up-regulating UbcH2/E220k. The FASEB Journal. **17**, 1048-1057
29 Li, Y.-P., Chen, Y., John, J., Moylan, J., Jin, B., Mann, D. L. and Reid, M. B. (2005) TNF-α acts via p38 MAPK to stimulate expression of the ubiquitin ligase atrogin1/MAFbx in skeletal muscle. The FASEB Journal. **19**, 362-370
30 Llovera, M., García-Martínez, C., Agell, N., López-Soriano, F. J. and Argilés, J. M. (1997) TNF can directly induce the expression of ubiquitin-dependent proteolytic system in rat soleus muscles. Biochemical and Biophysical Research Communications. **230**, 238-241
31 Llovera, M., Carbó, N., López-Soriano, J. n., García-Martínez, C., Busquets, S. l., Alvarez, B., Agell, N., Costelli, P., López-Soriano, F. J., Celada, A. and Argilés, J. M. (1998) Different cytokines modulate ubiquitin gene expression in rat skeletal muscle. Cancer Lett. **133**, 83-87
32 Cai, D., Frantz, J. D., Tawa, N. E., Melendez, P. A., Oh, B.-C., Lidov, H. G. W., Hasselgren, P.-O., Frontera, W. R., Lee, J., Glass, D. J. and Shoelson, S. E. (2004) IKKβ/NF-κB activation causes severe muscle wasting in mice. Cell. **119**, 285-298
33 Smith, H. J., Wyke, S. M. and Tisdale, M. J. (2004) Role of protein kinase C and NF-κB in proteolysis-inducing factor-induced proteasome expression in C2C12 myotubes. Br. J. Cancer. **90**, 1850
34 Whitehouse, A. S., Khal, J. and Tisdale, M. J. (2003) Induction of protein catabolism in myotubes by 15(S)-hydroxyeicosatetraenoic acid through increased expression of the ubiquitin–proteasome pathway. Br. J. Cancer. **89**, 737
35 Whitehouse, A. S. and Tisdale, M. J. (2003) Increased expression of the ubiquitin – proteasome pathway in murine myotubes by proteolysis-inducing factor (PIF) is associated with activation of the transcription factor NF-κB. Br. J. Cancer. **89**, 1116
36 Wyke, S. M., Russell, S. T. and Tisdale, M. J. (2004) Induction of proteasome expression in skeletal muscle is attenuated by inhibitors of NF-κB activation. Br. J. Cancer. **91**, 1742-1750
37 Al-Nassan, S., Fujita, N., Kondo, H., Murakami, S. and Fujino, H. (2012) Chronic exercise training down-regulates TNF-α and Atrogin-1/MAFbx in mouse gastrocnemius muscle atrophy induced by hindlimb unloading. Acta Histochem Cytochem. **45**, 343-349
38 Gleeson, M., Bishop, N. C., Stensel, D. J., Lindley, M. R., Mastana, S. S. and Nimmo, M. A. (2011) The anti-inflammatory effects of exercise: mechanisms and implications for the prevention and treatment of disease. Nature Reviews Immunology. **11**, 607
39 Kawanishi, N., Mizokami, T., Yano, H. and Suzuki, K. (2013) Exercise attenuates M1 macrophages and CD8+ T cells in the adipose tissue of obese mice. Med Sci Sports Exerc. **45**, 1684-1693

40 Bain, C. C., Bravo-Blas, A., Scott, C. L., Gomez Perdiguero, E., Geissmann, F., Henri, S., Malissen, B., Osborne, L. C., Artis, D. and Mowat, A. M. (2014) Constant replenishment from circulating monocytes maintains the macrophage pool in the intestine of adult mice. Nat. Immunol. **15**, 929
41 Hashimoto, D., Chow, A., Noizat, C., Teo, P., Beasley, Mary B., Leboeuf, M., Becker, Christian D., See, P., Price, J., Lucas, D., Greter, M., Mortha, A., Boyer, Scott W., Forsberg, E. C., Tanaka, M., van Rooijen, N., García-Sastre, A., Stanley, E. R., Ginhoux, F., Frenette, Paul S. and Merad, M. (2013) Tissue-resident macrophages self-maintain locally throughout adult life with minimal contribution from circulating monocytes. Immunity. **38**, 792-804
42 Robbins, C. S., Hilgendorf, I., Weber, G. F., Theurl, I., Iwamoto, Y., Figueiredo, J.-L., Gorbatov, R., Sukhova, G. K., Gerhardt, L. M. S., Smyth, D., Zavitz, C. C. J., Shikatani, E. A., Parsons, M., van Rooijen, N., Lin, H. Y., Husain, M., Libby, P., Nahrendorf, M., Weissleder, R. and Swirski, F. K. (2013) Local proliferation dominates lesional macrophage accumulation in atherosclerosis. Nat. Med. **19**, 1166
43 Krippendorf, B. B. and Riley, D. A. (1993) Distinguishing unloading. Versus reloading-induced changes in rat soleus muscle. Muscle Nerve. **16**, 99-108
44 Luster, A. D. (1998) Chemokines — Chemotactic cytokines that mediate inflammation. New England Journal of Medicine. **338**, 436-445
45 Warren, G. L., O'Farrell, L., Summan, M., Hulderman, T., Mishra, D., Luster, M. I., Kuziel, W. A. and Simeonova, P. P. (2004) Role of CC chemokines in skeletal muscle functional restoration after injury. Am. J. Physiol. Cell Physiol. **286**, C1031-1036
46 Warren, G. L., Hulderman, T., Mishra, D., Gao, X., Millecchia, L., O'Farrell, L., Kuziel, W. A. and Simeonova, P. P. (2005) Chemokine receptor CCR2 involvement in skeletal muscle regeneration. The FASEB Journal. **19**, 413-415
47 Hokeness, K. L., Kuziel, W. A., Biron, C. A. and Salazar-Mather, T. P. (2005) Monocyte chemoattractant protein-1 and CCR2 interactions are required for IFN-α/β-induced inflammatory responses and antiviral defense in liver. The Journal of Immunology. **174**, 1549-1556
48 Kasahara, T. and Matsushima, K. (2001) Macrophage signaling, apoptosis, lectins and leukocyte trafficking. Trends Immunol. **22**, 593-594
49 Takeda, K., Kaisho, T. and Akira, S. (2003) Toll-Like Receptors. Annu. Rev. Immunol. **21**, 335-376
50 Kobayashi, K., Kaneda, K. and Kasama, T. (2001) Immunopathogenesis of delayed-type hypersensitivity. Microsc. Res. Tech. **53**, 241-245
51 Maurice K. Gately, Louis M. Renzetti, Jeanne Magram, Alvin S. Stern, Adorini, L., Ueli Gubler, a. and Presky, D. H. (1998) The interleukin-12/interleukin-12-receptor system: Role in normal and pathologic immune responses. Annu. Rev. Immunol. **16**, 495-521
52 Rot, A. and Andrian, U. H. v. (2004) Chemokines in innate and adaptive host defense: Basic chemokinese grammar for immune cells. Annu. Rev. Immunol. **22**, 891-928
53 Arnold, L., Henry, A., Poron, F., Baba-Amer, Y., van Rooijen, N., Plonquet, A., Gherardi, R. K. and Chazaud, B. (2007) Inflammatory monocytes recruited after skeletal muscle injury switch into antiinflammatory macrophages to support myogenesis. J. Exp. Med. **204**, 1057-1069
54 Wynn, T. A. and Barron, L. (2010) Macrophages: master regulators of inflammation and fibrosis. Semin. Liver Dis. **30**, 245-257
55 Mantovani, A., Sica, A., Sozzani, S., Allavena, P., Vecchi, A. and Locati, M. (2004) The chemokine system in diverse forms of macrophage activation and polarization. Trends Immunol. **25**, 677-686
56 Wynn, T. A. (2004) Fibrotic disease and the Th_1/Th_2 paradigm. Nat. Rev. Immunol. **4**, 583-594
57 Biswas, S. K., Gangi, L., Paul, S., Schioppa, T., Saccani, A., Sironi, M., Bottazzi, B., Doni, A., Vincenzo, B., Pasqualini, F., Vago, L., Nebuloni, M., Mantovani, A. and Sica, A. (2006) A distinct and unique transcriptional program expressed by tumor-associated macrophages (defective NF-κB and enhanced IRF-3/STAT1 activation). Blood. **107**, 2112-2122
58 Wynn, T. A. (2008) Cellular and molecular mechanisms of fibrosis. J. Pathol. **214**, 199-210
59 Foster, D. F., Phillips, R. S., Hamel, M. B. and Eisenberg, D. M. (2000) Alternative medicine use in older americans. J. Am. Geriatr. Soc. **48**, 1560-1565
60 Moraska, A. (2007) Therapist education impacts the massage effect on postrace muscle recovery. Med Sci Sports Exerc. **39**, 34-37
61 Cafarelli, E. and Flint, F. (1992) The role of massage in preparation for and recovery from exercise. Sports Medicine. **14**, 1-9

62 Brummitt, J. (2008) The role of massage in sports performance and rehabilitation: Current evidence and future direction. North American Journal of Sports Physical Therapy : NAJSPT. **3**, 7-21
63 Netchanok, S., Wendy, M., Marie, C. and Siobhan, O. D. (2012) The effectiveness of swedish massage and traditional thai massage in treating chronic low back pain: A review of the literature. Complement. Ther. Clin. Pract. **18**, 227-234
64 Perlman, A. I., Sabina, A., Williams, A., Njike, V. and Katz, D. L. (2006) Massage therapy for osteoarthritis of the knee: A randomized controlled trial. Arch. Intern. Med. **166**, 2533-2538
65 Weerapong, P., Hume, P. A. and Kolt, G. S. (2005) The mechanisms of massage and Eefects on performance, muscle recovery and injury prevention. Sports Medicine. **35**, 235-256
66 Braverman, D. L. and Schulman, R. A. (1999) Massage techniques in rehabilitation medicine. Physical Medicine and Rehabilitation Clinics. **10**, 631-649
67 Bell, A. J. (1964) Massage and the physiotherapist. Physiotherapy. **50**, 406-408
68 Shoemaker, J. K., Tiidus, P. M. and Mader, R. (1997) Failure of manual massage to alter limb blood flow: measures by doppler ultrasound. Med Sci Sports Exerc. **29**, 610-614
69 Tiidus, P. M. and Shoemaker, J. K. (1995) Effleurage massage, muscle blood flow and long-term post-exercise strength recovery. Int J Sports Med. **16**, 478-483
70 Cara, D. C., Kaur, J., Forster, M., McCafferty, D.-M. and Kubes, P. (2001) Role of p38 mitogen-activated protein kinase in chemokine-induced emigration and chemotaxis in vivo. The Journal of Immunology. **167**, 6552-6558
71 Chambers, M. A., Moylan, J. S., Smith, J. D., Goodyear, L. J. and Reid, M. B. (2009) Stretch-stimulated glucose uptake in skeletal muscle is mediated by reactive oxygen species and p38 MAP-kinase. The Journal of Physiology. **587**, 3363-3373
72 Fan, H., Hall, P., Santos, L. L., Gregory, J. L., Fingerle-Rowson, G., Bucala, R., Morand, E. F. and Hickey, M. J. (2011) Macrophage migration inhibitory factor and CD74 regulate macrophage chemotactic responses via MAPK and Rho GTPase. The Journal of Immunology
73 Peake, J., Nosaka, K. and Suzuki, K. (2005) Characterization of inflammatory responses to eccentric exercise in humans. Exerc. Immunol. Rev. **11**, 64-85
74 Tidball, J. G. (2005) Inflammatory processes in muscle injury and repair. American Journal of Physiology-Regulatory, Integrative and Comparative Physiology. **288**, R345-R353
75 Crane, J. D., Ogborn, D. I., Cupido, C., Melov, S., Hubbard, A., Bourgeois, J. M. and Tarnopolsky, M. A. (2012) Massage therapy attenuates inflammatory signaling after exercise-induced muscle damage. Science translational medicine. **4**, 119ra113
76 Ironson, G., Field, T., Scafidi, F., Hashimoto, M., Kumar, M., Kumar, A., Price, A., Goncalves, A., Burman, I., Tetenman, C., Patarca, R. and Fletcher, M. A. (1996) Massage therapy is associated with enhancement of the immune system's cytotoxic capacity. Int. J. Neurosci. **84**, 205-217
77 Korosec, B. J. (2004) Manual lymphatic drainage therapy. Home Health Care Management & Practice. **16**, 499-511
78 Chikly, B. J. (2005) Manual techniques addressing the lymphatic system: origins and development. J. Am. Osteopath. Assoc. **105**, 457-464
79 Masson, I. F. B., de Oliveira, B. D. A., Machado, A. F. P., Farcic, T. S., Júnior, I. E. and Baldan, C. S. (2014) Manual lymphatic drainage and therapeutic ultrasound in liposuction and lipoabdominoplasty post-operative period. Indian Journal of Plastic Surgery : Official Publication of the Association of Plastic Surgeons of India. **47**, 70-76
80 Lee, I. M., Shiroma, E. J., Lobelo, F., Puska, P., Blair, S. N. and Katzmarzyk, P. T. (2012) Effect of physical inactivity on major non-communicable diseases worldwide: an analysis of burden of disease and life expectancy. Lancet (London, England). **380**, 219-229
81 Berg, H. E., Larsson, L. and Tesch, P. A. (1997) Lower limb skeletal muscle function after 6 wk of bed rest. Journal of Applied Physiology. **82**, 182-188
82 Caron, A. Z., Drouin, G., Desrosiers, J., Trensz, F. and Grenier, G. (2009) A novel hindlimb immobilization procedure for studying skeletal muscle atrophy and recovery in mouse. J Appl Physiol (1985). **106**, 2049-2059
83 Hunter, R. B., Stevenson, E., Koncarevic, A., Mitchell-Felton, H., Essig, D. A. and Kandarian, S. C. (2002) Activation of an alternative NF-κB pathway in skeletal muscle during disuse atrophy. FASEB J. **16**, 529-538
84 Winkelman, C. (2004) Inactivity and inflammation: selected cytokines as biologic mediators in muscle dysfunction during critical illness. AACN clinical issues. **15**, 74-82

85 Lira, F. S., Koyama, C. H., Yamashita, A. S., Rosa, J. C., Zanchi, N. E., Batista, M. L., Jr. and Seelaender, M. C. (2009) Chronic exercise decreases cytokine production in healthy rat skeletal muscle. Cell Biochem Funct. **27**, 458-461
86 Dogra, S., Ashe, M. C., Biddle, S. J. H., Brown, W. J., Buman, M. P., Chastin, S., Gardiner, P. A., Inoue, S., Jefferis, B. J., Oka, K., Owen, N., Sardinha, L. B., Skelton, D. A., Sugiyama, T. and Copeland, J. L. (2017) Sedentary time in older men and women: an international consensus statement and research priorities. Br. J. Sports Med. **51**, 1526-1532
87 Hamilton, M. T., Healy, G. N., Dunstan, D. W., Zderic, T. W. and Owen, N. (2008) Too little exercise and too much sitting: inactivity physiology and the need for new recommendations on sedentary behavior. Current cardiovascular risk reports. **2**, 292-298
88 Furlan, A. D., Giraldo, M., Baskwill, A., Irvin, E. and Imamura, M. (2015) Massage for low-back pain. The Cochrane database of systematic reviews, Cd001929
89 Robertson, A., Watt, J. and Galloway, S. (2004) Effects of leg massage on recovery from high intensity cycling exercise. Br. J. Sports Med. **38**, 173-176
90 Waters-Banker, C., Butterfield, T. A. and Dupont-Versteegden, E. E. (2014) Immunomodulatory effects of massage on nonperturbed skeletal muscle in rats. Journal of Applied Physiology. **116**, 164-175
91 Haas, C., Butterfield, T. A., Abshire, S., Zhao, Y., Zhang, X., Jarjoura, D. and Best, T. M. (2013) Massage timing affects postexercise muscle recovery and inflammation in a rabbit model. Med Sci Sports Exerc. **45**, 1105-1112
92 Stewart, L. K., Flynn, M. G., Campbell, W. W., Craig, B. A., Robinson, J. P., Timmerman, K. L., McFarlin, B. K., Coen, P. M. and Talbert, E. (2007) The influence of exercise training on inflammatory cytokines and C-reactive protein. Med Sci Sports Exerc. **39**, 1714-1719
93 Timmerman, K. L., Flynn, M. G., Coen, P. M., Markofski, M. M. and Pence, B. D. (2008) Exercise training-induced lowering of inflammatory ($CD14^+CD16^+$) monocytes: a role in the anti-inflammatory influence of exercise? J Leukoc Biol. **84**, 1271-1278
94 Acharyya, S., Villalta, S. A., Bakkar, N., Bupha-Intr, T., Janssen, P. M. L., Carathers, M., Li, Z.-W., Beg, A. A., Ghosh, S., Sahenk, Z., Weinstein, M., Gardner, K. L., Rafael-Fortney, J. A., Karin, M., Tidball, J. G., Baldwin, A. S. and Guttridge, D. C. (2007) Interplay of IKK/NF-κB signaling in macrophages and myofibers promotes muscle degeneration in duchenne muscular dystrophy. The Journal of Clinical Investigation. **117**, 889-901
95 Kang, X., Hou, A., Wang, R., Liu, D., Xiang, W., Xie, Q., Zhang, B., Gan, L., Zheng, W. and Miao, H. (2016) Macrophage TCF-4 co-activates p65 to potentiate chronic inflammation and insulin resistance in mice. Clinical Science. **130**, 1257-1268
96 Kirstein, M., Brett, J., Radoff, S., Ogawa, S., Stern, D. and Vlassara, H. (1990) Advanced protein glycosylation induces transendothelial human monocyte chemotaxis and secretion of platelet-derived growth factor: role in vascular disease of diabetes and aging. Proceedings of the National Academy of Sciences. **87**, 9010-9014
97 Yasojima, K., Schwab, C., McGeer, E. G. and McGeer, P. L. (2001) Complement components, but not complement inhibitors, are upregulated in atherosclerotic plaques. Arteriosclerosis, Thrombosis, and Vascular Biology. **21**, 1214-1219
98 L., M. P. and G., M. E. (2004) Inflammation and the degenerative diseases of Aaing. nnals of the New York Academy of Sciences. **1035**, 104-116
99 Simpson, E. R. and Brown, K. A. (2013) Minireview: Obesity and breast cancer: a tale of inflammation and dysregulated metabolism. Molecular endocrinology (Baltimore, Md.). **27**, 715-725
100 Akiko, O., Hajime, K., Qibin, J., Takayuki, A., Toshikazu, M., Yasuhiro, S., Katsuhiko, S., Yoichiro, K., Susumu, M. and Toru, F. (2016) New mouse model of skeletal muscle atrophy using spiral wire immobilization. Muscle Nerve. **54**, 788-791
101 Mori, Y., Chen, T., Fujisawa, T., Kobashi, S., Ohno, K., Yoshida, S., Tago, Y., Komai, Y., Hata, Y. and Yoshioka, Y. (2014) From cartoon to real time MRI: in vivo monitoring of phagocyte migration in mouse brain. Scientific Reports. **4**, 6997
102 Ma, Y., Li, Y., Jiang, L., Wang, L., Jiang, Z., Wang, Y., Zhang, Z. and Yang, G.-Y. (2016) Macrophage depletion reduced brain injury following middle cerebral artery occlusion in mice. J. Neuroinflammation. **13**, 38
103 Strober, W. (2000) Wright-Giemsa and nonspecific esterase staining of cells. Current Protocols in Cytometry. **11**, A.3D.1-A.3D.4

104 Lee, S. H., Starkey, P. M. and Gordon, S. (1985) Quantitative analysis of total macrophage content in adult mouse tissues. Immunochemical studies with monoclonal antibody F4/80. The Journal of Experimental Medicine. **161**, 475-489
105 Ogasawara, R., Kobayashi, K., Tsutaki, A., Lee, K., Abe, T., Fujita, S., Nakazato, K. and Ishii, N. (2013) mTOR signaling response to resistance exercise is altered by chronic resistance training and detraining in skeletal muscle. Journal of Applied Physiology. **114**, 934-940
106 Reid, M. B. and Li, Y.P. (2001) Tumor necrosis factor-α and muscle wasting: a cellular perspective. Respiratory Research. **2**, 269
107 Rolf, K. R. (1981) Interstitial fluid volume, colloid osmotic and hydrostatic pressures in rat skeletal muscle. Effect of venous stasis and muscle activity. Acta Physiologica Scandinavica. **112**, 7-17
108 Van Rooijen, N. (1989) The liposome-mediated macrophage 'suicide' technique. Journal of Immunological Methods. **124**, 1-6
109 Côté, C. H., Bouchard, P., Van Rooijen, N., Marsolais, D. and Duchesne, E. (2013) Monocyte depletion increases local proliferation of macrophage subsets after skeletal muscle injury. BMC Musculoskeletal Disorders. **14**, 359
110 Zurovsky, Y., Mitchell, G., Hattingh, J. (1995) Composition and viscosity of interstitial fluid of rabbits. Experimental Physiology. **80**, 203-207
111 Shorten, P. R., McMahon, C. D. and Soboleva, T. K. (2007) Insulin transport within skeletal muscle transverse tubule networks. Biophysical Journal. **93**, 3001-3007
112 Ghosn, E. E., Cassado, A. A., Govoni, G. R., Fukuhara, T., Yang, Y., Monack, D. M., Bortoluci, K. R., Almeida, S. R., Herzenberg, L. A. and Herzenberg, L. A. (2010) Two physically, functionally, and developmentally distinct peritoneal macrophage subsets. Proc Natl Acad Sci U S A. **107**, 2568-2573
113 Lu, H.-L., Huang, X.-Y., Luo, Y.-F., Tan, W.-P., Chen, P.-F. and Guo, Y.-B. (2018) Activation of M1 macrophages plays a critical role in the initiation of acute lung injury. Biosci. Rep. **38**, BSR20171555
114 H., F. A. and A., F. L. (1994) Isolation of murine macrophages. Current Protocols in Immunology. **11**, 14.11.11-14.11.19
115 Jenkins, S. J., Ruckerl, D., Cook, P. C., Jones, L. H., Finkelman, F. D., van Rooijen, N., MacDonald, A. S. and Allen, J. E. (2011) Local macrophage proliferation, rather than recruitment from the blood, is a signature of Th_2 inflammation. Science. **332**, 1284-1288
116 D., S. W., M., K. R., K., G. J., Juozas, V., A., L. M. and E., W. S. (2011) Ron receptor regulates Kupffer cell−dependent cytokine production and hepatocyte survival following endotoxin exposure in mice. Hepatology. **53**, 1618-1628
117 Yoshino, D., Sakamoto, N., Takahashi, K., Inoue, E. and Sato, M. (2013) Development of novel flow chamber to study endothelial cell morphology: effects of shear flow with uniform spatial gradient on distribution of focal adhesion. Journal of Biomechanical Science and Engineering. **8**, 233-243
118 Yoshino, D., Sato, K. and Sato, M. (2015) Endothelial cell response under hydrostatic pressure condition mimicking pressure therapy. Cellular and Molecular Bioengineering. **8**, 296-303
119 Porcheray, F., Viaud, S., Rimaniol, A.-C., Léone, C., Samah, B., Dereuddre-Bosquet, N., Dormont, D. and Gras, G. (2005) Macrophage activation switching: an asset for the resolution of inflammation. Clinical & Experimental Immunology. **142**, 481-489
120 Sanjabi, S., Zenewicz, L. A., Kamanaka, M. and Flavell, R. A. (2009) Anti-inflammatory and pro-inflammatory roles of TGF-β, IL-10, and IL-22 in immunity and autoimmunity. Current Opinion in Pharmacology. **9**, 447-453
121 Malek, A. M., Alper, S. L. and Izumo, S. (1999) Hemodynamic shear stress and its role in atherosclerosis. JAMA. **282**, 2035-2042
122 Wehner, S., Buchholz, B. M., Schuchtrup, S., Rocke, A., Schaefer, N., Lysson, M., Hirner, A. and Kalff, J. C. (2010) Mechanical strain and TLR4 synergistically induce cell-specific inflammatory gene expression in intestinal smooth muscle cells and peritoneal macrophages. American Journal of Physiology-Gastrointestinal and Liver Physiology. **299**, G1187-G1197
123 Maruyama, K., Sakisaka, Y., Suto, M., Tada, H., Nakamura, T., Yamada, S. and Nemoto, E. (2018) Cyclic stretch negatively regulates IL-1β secretion through the inhibition of NLRP3 inflammasome activation by attenuating the AMP kinase pathway. Front. Physiol. **9**

124 Sawada, Y., Nakamura, K., Doi, K., Takeda, K., Tobiume, K., Saitoh, M., Morita, K., Komuro, I., De Vos, K., Sheetz, M. and Ichijo, H. (2001) Rap1 is involved in cell stretching modulation of p38 but not ERK or JNK MAP kinase. Journal of Cell Science. **114**, 1221-1227
125 Davies, B. and Morris, T. (1993) Physiological parameters in laboratory animals and humans. Pharmaceutical Research. **10**, 1093-1095
126 Benias, P. C., Wells, R. G., Sackey-Aboagye, B., Klavan, H., Reidy, J., Buonocore, D., Miranda, M., Kornacki, S., Wayne, M., Carr-Locke, D. L. and Theise, N. D. (2018) Structure and distribution of an unrecognized interstitium in human tissues. Scientific Reports. **8**, 4947
127 Jéquier, E. and Constant, F. (2009) Water as an essential nutrient: the physiological basis of hydration. European Journal Of Clinical Nutrition. **64**, 115
128 Bonewald, L. F. (2006) Mechanosensation and transduction in osteocytes. IBMS BoneKEy. **3**, 7-15
129 McDermott, A. G. P., Marble, A. E., Yabsley, R. H. and Phillips, M. B. (1982) Monitoring dynamic anterior compartment pressures during exercise:A new technique using the STIC catheter. The American Journal of Sports Medicine. **10**, 83-89
130 Discher, D., Dong, C., Fredberg, J. J., Guilak, F., Ingber, D., Janmey, P., Kamm, R. D., Schmid-Schönbein, G. W. and Weinbaum, S. (2009) Biomechanics: Cell research and applications for the next decade. Ann. Biomed. Eng. **37**, 847
131 Yamawaki, H., Pan, S., Lee, R. T. and Berk, B. C. (2005) Fluid shear stress inhibits vascular inflammation by decreasing thioredoxin-interacting protein in endothelial cells. The Journal of Clinical Investigation. **115**, 733-738
132 Kovacs, G., Berghold, A., Scheidl, S. and Olschewski, H. (2009) Pulmonary arterial pressure during rest and exercise in healthy subjects: a systematic review. European Respiratory Journal. **34**, 888-894
133 Y, K. R., R, M. D., Joyce, T. W. and A, F. J. (2010) Microfluidic enhancement of intramedullary pressure increases interstitial fluid flow and inhibits bone loss in hindlimb suspended mice. Journal of Bone and Mineral Research. **25**, 1798-1807
134 Best, T. M., Hunter, R., Wilcox, A. and Haq, F. (2008) Effectiveness of sports massage for recovery of skeletal muscle from strenuous exercise. Clinical Journal of Sport Medicine. **18**, 446-460
135 Lucitti, J. L., Jones, E. A., Huang, C., Chen, J., Fraser, S. E. and Dickinson, M. E. (2007) Vascular remodeling of the mouse yolk sac requires hemodynamic force. Development. **134**, 3317-3326
136 Orr, A. W., Helmke, B. P., Blackman, B. R. and Schwartz, M. A. (2006) Mechanisms of mechanotransduction. Dev. Cell. **10**, 11-20
137 Givens, C. and Tzima, E. (2016) Endothelial Mechanosignaling: does one sensor fit all? Antioxid. Redox Signal. **25**, 373-388
138 Springer, N. L. and Fischbach, C. (2016) Biomaterials approaches to modeling macrophage-extracellular matrix interactions in the tumor microenvironment. Curr. Opin. Biotechnol. **40**, 16-23
139 Multhaupt, H. A., Leitinger, B., Gullberg, D. and Couchman, J. R. (2016) Extracellular matrix component signaling in cancer. Adv Drug Deliv Rev. **97**, 28-40
140 Parekh, A. and Weaver, A. M. (2016) Regulation of invadopodia by mechanical signaling. Exp. Cell Res. **343**, 89-95
141 Yu, F. X., Zhao, B. and Guan, K. L. (2015) Hippo pathway in organ size control, tissue homeostasis, and cancer. Cell. 163, 811-828
142 Tarbell, J.M. and Shi, Z.D. (2013) Effect of the glycocalyx layer on transmission of interstitial flow shear stress to embedded cells. Biomech. Model. Mechanobiol. 12, 111-121

Chapter 8

Acknowledgements

Chapter 8. Acknowledgments

I would like to thank all members of the preventive medicine laboratory. Dr. Kawanishi, Dr. Yada gave me advice on my experiments. This study was supported by National Rehabilitation Center for Persons with Disabilities, I would like to be grateful to all members of National Rehabilitation Center for Persons with Disabilities, Dr. Tokunaga, Dr. Sakitani, Dr. Maekawa, Dr. Ryu, Dr. Nagao, Dr. Ogata and Dr. Ichihara. Thanks to their supports, I was able to finish writing this doctoral dissertation. In particular, I would like to thank Professor Katsuhiko Suzuki and Doctor Yasuhiro Sawada whose enthusiastic guidance including various advices, many supports, valuable discussion and considerable encouragement made my research high quality.